Supporting information

Importance of small loops within PIM-1 topology on gas separation selectivity in thin film composite membranes

Andrew B. Foster[a,*], Joseph L. Beal[a], Marzieh Tamaddondar[a], Jose Miguel Luque-Alled[b], Ben Robertson[a], Michael Mathias[a], Patricia Gorgojo[b], Peter M. Budd[a,*]

[a]Department of Chemistry, The University of Manchester, Oxford Road, Manchester, M13 9PL, UK.

[b]Department of Chemical Engineering and Analytical Science, The University of Manchester, M13 9PL, UK.

Corresponding authors:

* The University of Manchester. Oxford Road, Manchester M13 9PL, UK. Emails: peter.budd@manchester.ac.uk & andrew.foster@manchester.ac.uk; Tel: +44(0)1612754711.

INDEX

S1. Materials.

The monomers, 5,5'6,6'-tetrahydroxy-3,3,3',3'-tetramethyl-1,1'-spirobisindane (TTSBI) and tetrachloroterephthalonitrile (TCTPN), were purchased from Alfa Aesar and Jinan Finer Chemical Co. Ltd (China), respectively, and were used as received at certified levels of purity, after drying in vacuum overnight at room temperature. Anhydrous potassium carbonate was purchased from Fisher Scientific Ltd, with the base ground into a fine powder and dried in a vacuum oven at 110 °C overnight before use. Anhydrous dimethylacetamide, (DMAc), anhydrous 1,2-dichlorobenzene, (DCB), methanol, chloroform, tetrahydrofuran and 1,4-dioxane were purchased from Sigma-Aldrich and used as received.

S2. Purification of PIM-1 polymer.

The recovered filtered polymer was re-dissolved in chloroform at a concentration of ca. 5 g / 120 ml and then re-precipitated by pouring slowly into methanol. The PIM-1 polymer was collected via filtration and then refluxed in de-ionized water for 16 hours. The filtered polymer was immersed in a minimal amount of 1,4-dioxane for 15 min (volume of dioxane used was just enough to cover the mass of polymer in the beaker). The polymer was then filtered before washing further with copious amounts of acetone. The filtered polymer was left to soak in methanol overnight to remove all traces of dioxane and acetone. It was then filtered dry using a sintered glass funnel with vacuum before being dried in a vacuum oven at 120 °C for 2 days to completely remove all traces all solvent. The polymer yields reported in Table 1 are after this purification process.

S3. Characterization.

^{1}H and ^{13}C nuclear magnetic resonance (NMR) spectra of PIM-1 polymers were recorded using a Bruker Avance II 500 MHz instrument. 50 mg ml^{-1} polymer solutions in CDCl$_3$ were prepared for the NMR analysis (Schemes S1 & S2, Figures S1-S8 in supporting information). Signal peaks for the solvent were used as references.

Average molar masses of the PIM-1 polymers were measured by triple detector size exclusion chromatography (SEC). Analysis was performed in chloroform from 1 mg ml^{-1} polymer solutions (injection volume 100 µL) at a flow rate of 1 mL min^{-1} using a Viscotek VE2001 SEC solvent / sample module with two PL Mixed B columns and a Viscotek TDA 302 triple detector array (refractive index, light scattering, viscosity detectors). The data were analysed in OmniSec software. A polystyrene standard of known molar mass (110 kg mol^{-1}) was used for system calibration.

A Flash 2000 Organic Elemental Analyser (Thermo Scientific, The Netherlands) was employed to obtain elemental analysis data. 5 mg of powder was used for each experiment.

MALDI-TOF mass spec analysis was completed on a Shimadzu Biotech Axima Confidence instrument. Each sample of approximately 5 mg was dissolved in chloroform (100 µL). The chloroform solution was then mixed with a matrix solution (dithranol in THF, 10 mg ml^{-1}) in a 1 : 10 ratio (sample : matrix). This resultant mixture was then spotted onto a plate using the layered method with sodium iodide solution (10 mg ml^{-1}). Calibration was completed using a spherical peptide mix at a range of 1600-3500 Da. Samples were run with the instrument in linear mode with the pulse extraction optimised at 7000 kg mol^{-1}.

UV–vis absorption spectra were recorded on a Varian Cary 5000 UV–vis–NIR spectrophotometer from polymer solutions prepared in THF (0.09 mM) at room temperature.

Dynamic light scattering (DLS) analysis of PIM-1 sample dispersions (50 ppm) in chloroform at 25 °C were completed on a Malvern Zetasizer Nano ZS instrument.

Micromeritics ASAP 2020 was used to obtain N$_2$ adsorption/desorption isotherms at 77 K and to measure the Brunauer-Emmett-Teller (BET) surface area. Samples were accurately weighed and about 0.10 g of the polymer

was degassed at 120 °C for 16 h under high vacuum (10-5 bar) before starting the analysis at 77.3 K. After cooling, degassed samples were reweighed, and placed in the analysis port. Nitrogen adsorption/desorption isotherms were undertaken at 77 K. Helium was used for the free space determination before sorption analysis.

Polymer thermal degradation curves were obtained from thermogravimetric analysis (TGA) with a TGA Perkin-Elmer System. Polymer samples for TGA were initially heated at 10 °C/min up to 150 °C under nitrogen atmosphere and then maintained at that temperature for 1 h for moisture removal before being heated to 600 °C at 10 °C/min for degradation temperature measurement.

S4. Transmission electron microscopy (TEM) preparation and analysis of thin film composites.

TEM analysis was carried out using a FEI Tecnai G2 20 microscope operating at 200 kV. Thin film membrane samples were embedded in epoxy resin and further underwent ultramicrotomy with the aim of obtaining ultra-thin specimens of 100 nm. Ultracut E ultramicrotome (Reichert-Jung, USA) and a diamond knife purchased from DiATOME (Switzerland) were used for the process described below. Araldite resin AY103-1 and Aradur hardener HY951 were used as resin precursors, both were mixed in 10:1 ratio and poured into a silicon rubber mold. Then, the membrane samples were immersed in the mixture and left to dry under N_2 flow for 24 hours at room temperature. The dried piece of resin was first polished in order to obtain a pyramid-like shape. Afterwards, an ultramicrotome trimming process of the sample was carried out with a glass diamond knife to create a narrower and clean window. Finally, ultra-thin specimens were obtained using the diamond knife positioned perpendicular to the face of the membrane specimen. During the cutting process, the diamond knife was tilted at an angle of 6° and the speed set at 1 mm s^{-1}. The specimens were removed from the water by means of a lacey carbon film on mesh copper grid and further dried at room temperature for 2 hours.

S5. Roller coater process.
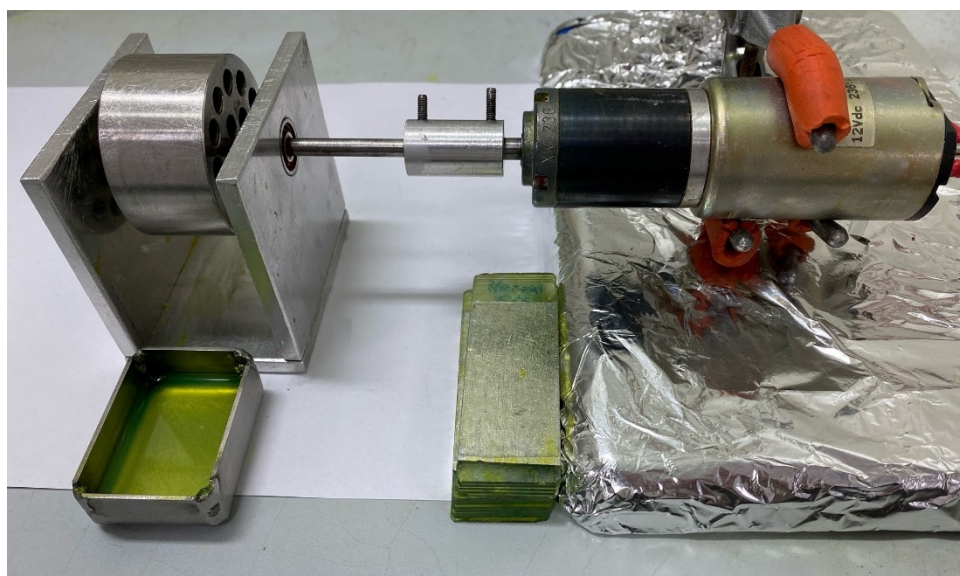
Once a piece of PAN support (25 × 60 mm) was adhered to the top of the roller wheel, with all edges sealed with aluminium tape, a bucket containing the polymer solution (0.3 g in 10 ml chloroform) was placed directly underneath the roller wheel. The level of the bucket was then adjusted by placing a group of microscope slides underneath it, sufficient to mean that the bottom of the roller wheel was just in contact with the chloroform solution. The roller completed one full rotation with the PAN support in direct contact with the underlying solution for about 2 s. The remaining chloroform solution in the bucket was quickly decanted into a sample bottle and sealed ready for re-use. The PIM-1 coated PAN support strip was detached from the roller and placed flat to dry for 24 h in a nitrogen atmosphere storage cabinet before commencement of testing. Each single strip provided two coupons for use in the single gas permeation rig. Both the roller wheel and the bucket were then

cleaned of PIM-1 polymer film. The process was repeated with a new piece of PAN support (25 x 60 mm) and the remaining chloroform solution poured into a clean bucket. If necessary an additional microscope slide was placed under the bucket to ensure that the solution was in contact with the roller wheel prior to the single rotation through the solution. It was found that generally this process could be repeated to coat a total of 5 separate strips before the solution remaining in the bucket proved insufficient to uniformly coat the surface of the PAN support. This meant that a total of 10 coupons (5 ×2) were generally prepared from each chloroform solution for gas permeation testing. At least two coupons, selected from separate strips, were used in the determination of each aging interval measurement. Enough coupons were prepared such that they did not need to be reused in the testing process. The coupons could be retested, if required, to give more data at longer aging intervals. An initial test of the reproducibility of the coating process was completed with a single PIM-1 blend solution (2 wt % of polymer **3** in polymer **1**, **Table S8**) which involved testing all 8 coupons generated from 4 different strips after 1 day aging. Consistent permeances of carbon dioxide and nitrogen of 4349 (±367) GPU and 305 (±40) GPU respectively were recorded across the range of coupons. The standard deviations obtained compared favourably against that noted for gas permeation analysis of self-standing PIM-1 films.

S6. Single gas permeation measurements.

The permeability measurements using single gases (CO_2 and N_2) were carried out by the standard variable volume method[20] at a gauge pressure of approximately 2 atm for each single gas at ambient temperature (~ 298 K) and the permeate side was at atmospheric pressure. Membrane samples (25 mm in diameter), were immediately mounted in the permeation cell. The gas permeance was calculated using:

$$K = \frac{Q}{tA(p_1 - p_2)} \cdot 10^{-6}$$

where K is the permeance in gas permeation units (1 GPU = 10^{-6} cm^3[STP] cm^{-2} s^{-1} cmHg^{-1} = 3.348×10^{-10} mol m^{-2} s^{-1} Pa^{-1}), Q is the volume of permeated gas (cm^3, adjusted to STP [0 °C, 1 atm]), t is the permeation time (s), A is the membrane area (cm^2), and p_1 and p_2 are the feed and permeate side pressures (cmHg), respectively. Gas permeability was calculated using:

$$P = \frac{Q\, l}{tA(p_1 - p_2)} \cdot 10^{-10}$$

where l is the membrane thickness (cm) and P is the permeability coefficient expressed in barrer (1 barrer = 10^{-10} cm^3[STP] cm cm^{-2} s^{-1} cmHg^{-1} = 3.348×10^{-16} mol m m^{-2} s^{-1} Pa^{-1}).

Main chain NMR analysis:
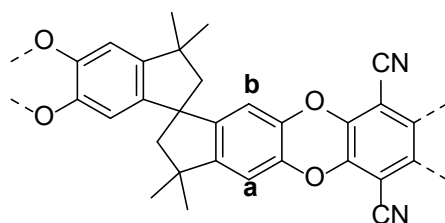
End group NMR analysis:
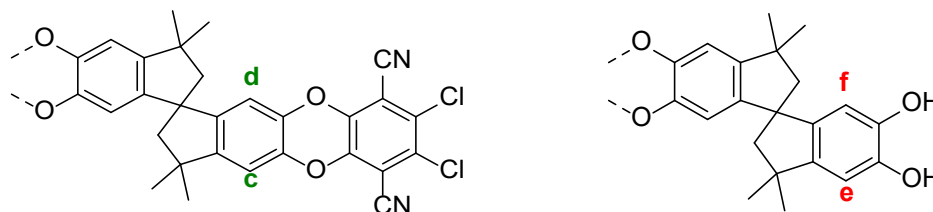
Under-reacted and branched NMR analysis:
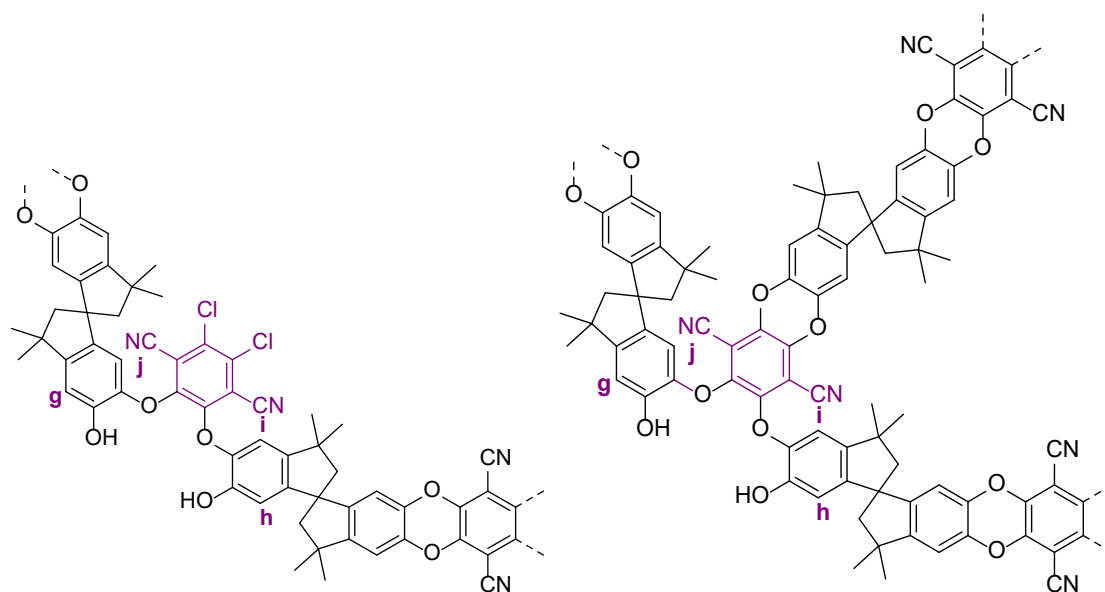
Scheme S1. ^{1}H NMR spectral assignments of key aromatic protons in PIM-1 microstructures.

PIM-1 proton NMR assignments:

Main chain PIM-1 resonances (δ, ^{1}H NMR, CDCl$_3$): aromatic C**H** × 4 (2H$_a$ and 2H$_b$), 6.81 & 6.42 ppm, aliphatic C**H$_2$** × 2 (4H), 2.33 & 2.16 ppm, aliphatic C**H$_3$** × 4 (12H) 1.37 & 1.31 ppm.

End group / other ^{1}H NMR resonances (δ, ^{1}H NMR, CDCl$_3$): aromatic C**H** × 4 (2H$_c$ and 2H$_d$), 6.88 & 6.48 ppm, aromatic C**H** × 4 (2H$_e$ and 2H$_f$), unresolved & 5.85 ppm, aromatic C**H** × 4 (2H$_g$ and 2H$_h$), 6.66 & 6.27 ppm.
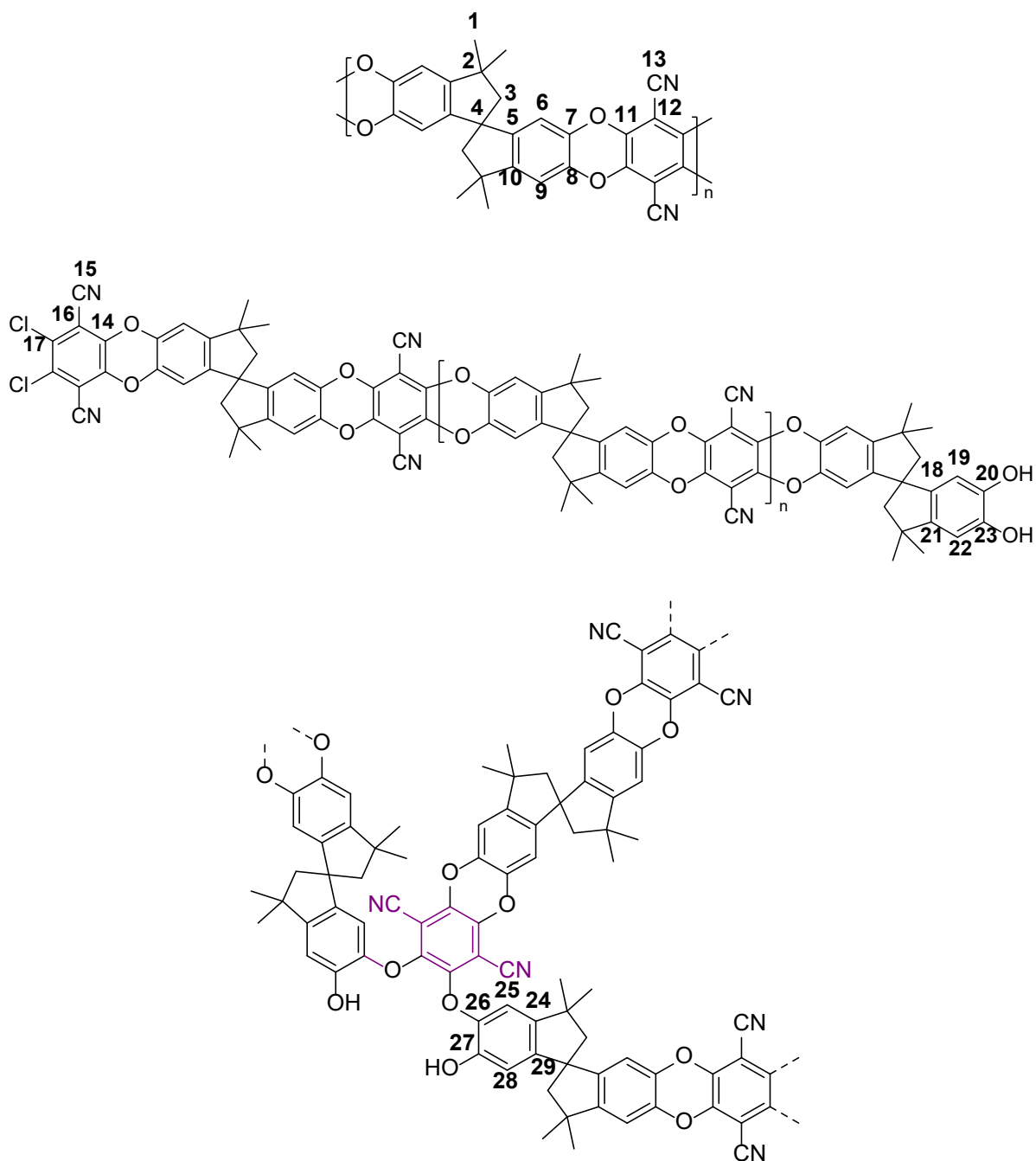
Scheme S2. ^{13}C NMR spectral analysis labelling of PIM-1 polymers.

PIM-1 carbon NMR assignments:

PIM-1 (δ, ^{13}C NMR, CDCl$_3$): aromatic **C** $\times$ 7, 149.8 (**5**), 147.1 (**10**), 139.6 & 139.3 (**7, 8, 11**), 112.4 (**13**), 110.7 (**9**), 109.5 (**6**) ppm, (CN)**C** 94.3 ppm (**12**), **C**H$_2$ 59.0 ppm (**3**), **C** 57.3 ppm (**4**), (CH$_3$)$_2$**C** 43.7 ppm (**2**), **C**H$_3$ 31.5 & 30.1 ppm (**1**).

End group / other ^{13}C NMR resonances: 150.6(**23**), 147.8 (**20**), 146.9, 146.2, 144.9 (**14**), 143.6, 129.5 (**17**), 112.8(**15**), 111.0, 110.5, 106.4 (**16**)
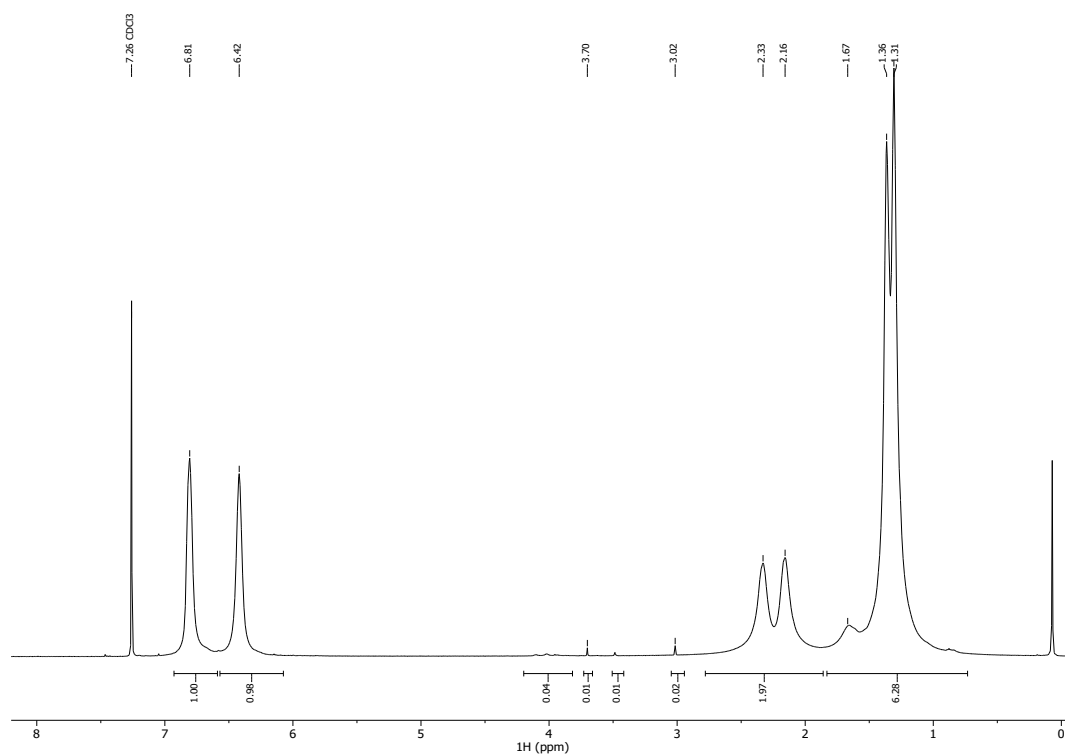
Figure S1. ^1H NMR spectrum of PIM-1 sample from reaction **1** at 140 °C under excessive N_2 purge conditions (**Table 1**).
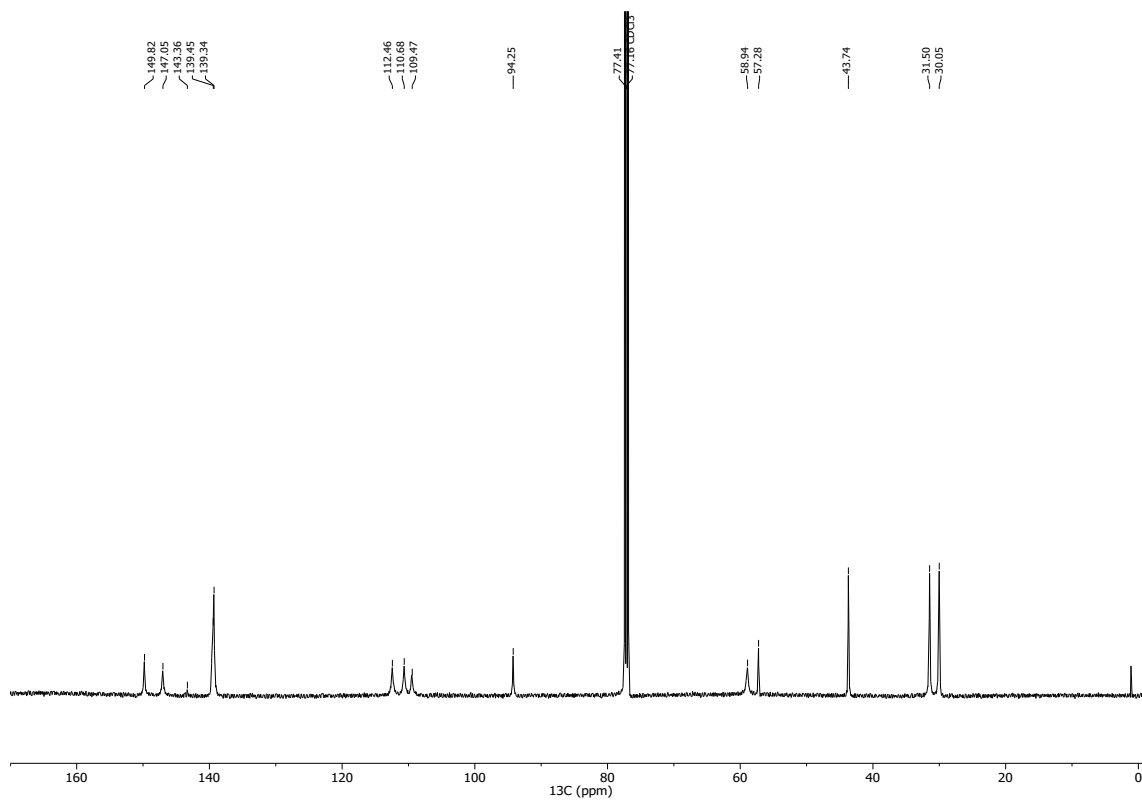
Figure S2. ^{13}C NMR spectrum of PIM-1 sample from reaction **1** at 140 °C under excessive N_2 purge conditions (**Table 1**).
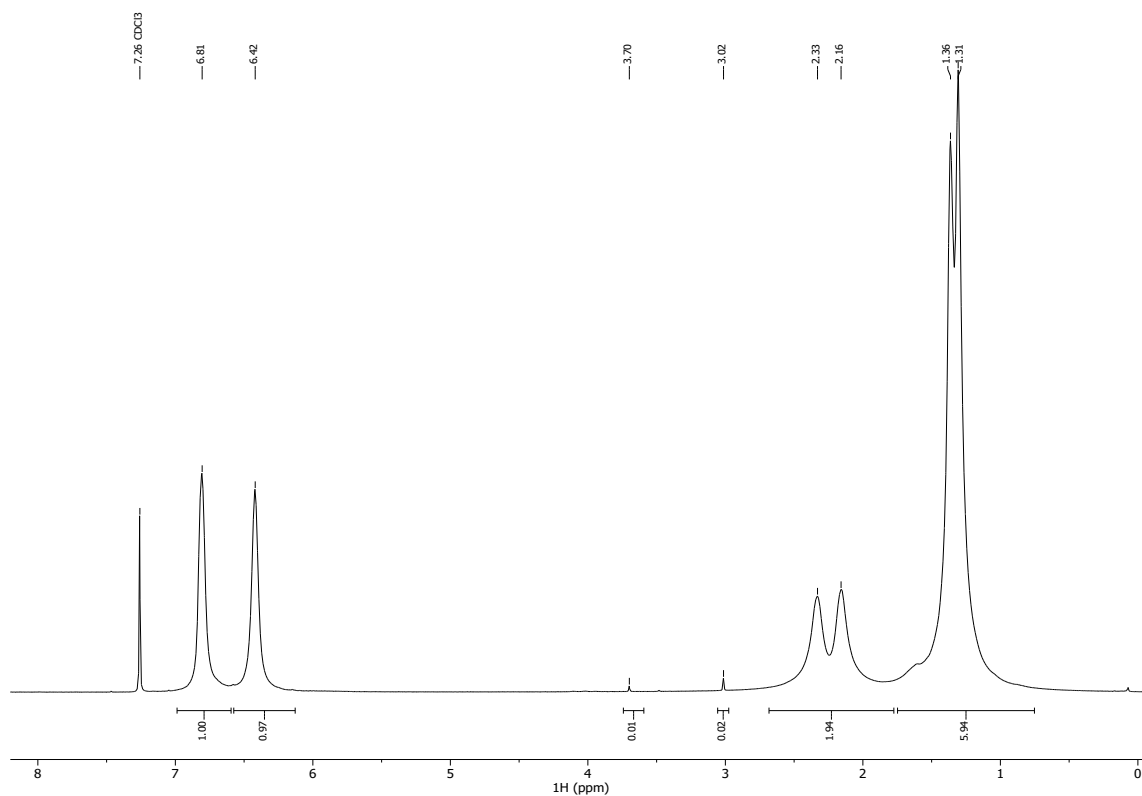
Figure S3. ^{1}H NMR spectrum of PIM-1 sample from reaction **2** at 120 °C under excessive N_2 purge conditions (**Table 1**).
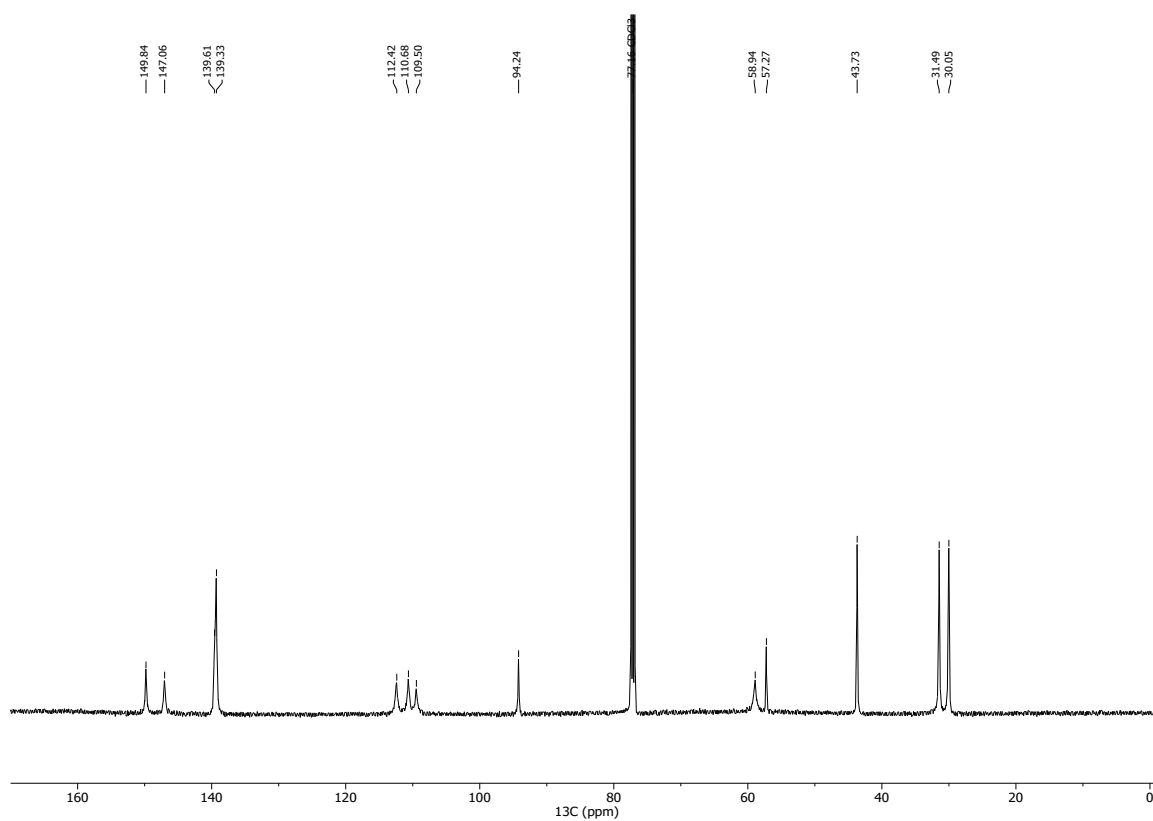
Figure S4. ^{13}C NMR spectrum of PIM-1 sample from reaction **2** at 120 °C under excessive N_2 purge conditions (**Table 1**).
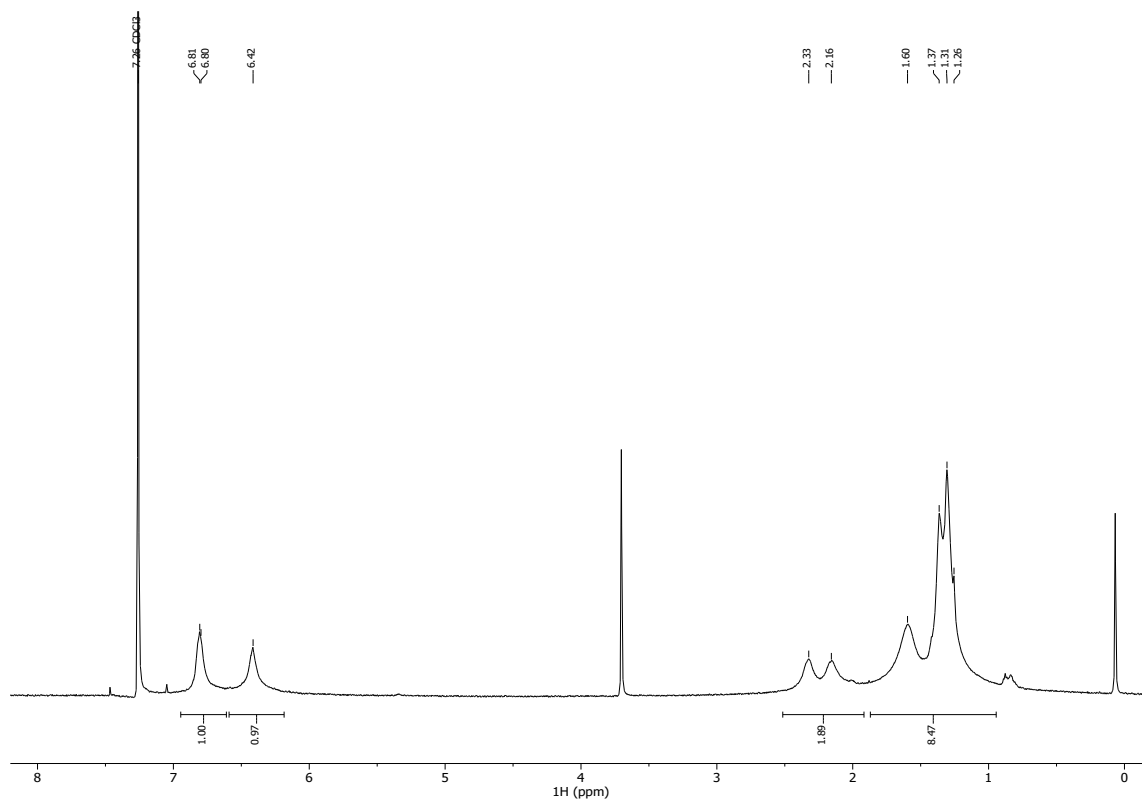
Figure S5. ^{1}H NMR spectrum of PIM-1 sample from reaction **3** at 160 °C in air (no inert gas) (**Table 1**).
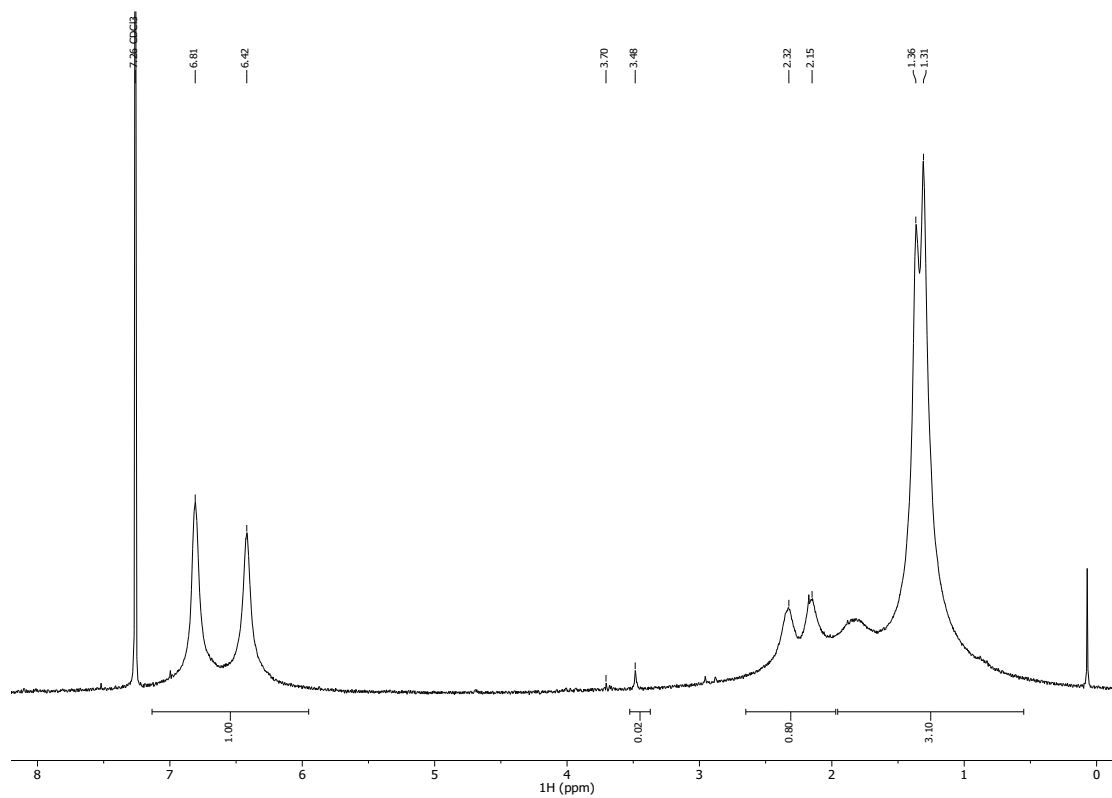
Figure S6. ^{1}H NMR spectrum of PIM-1 sample from reaction **4** at 140 °C in air (no inert gas (**Table 1**).
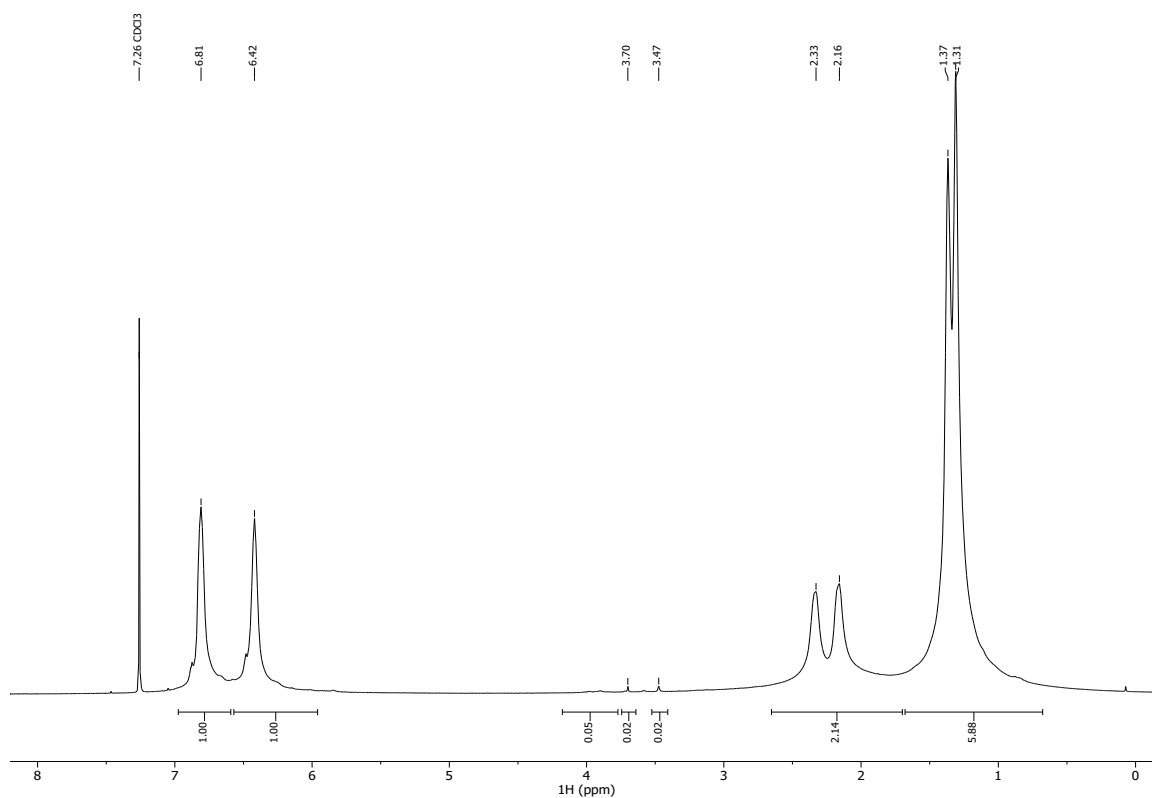
Figure S7. ^{1}H NMR spectrum of PIM-1 sample from reaction **5** at 120 °C in air (no inert gas) (**Table 1**).
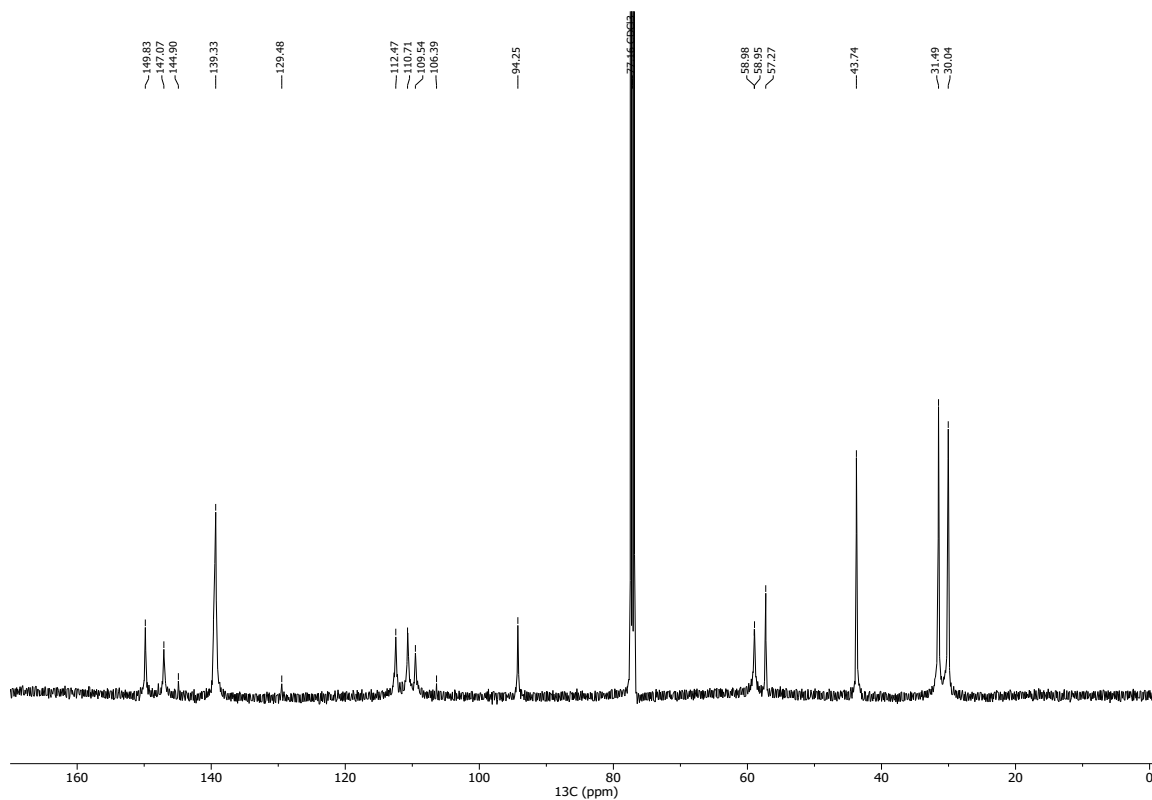
Figure S8. ^{13}C NMR spectrum of PIM-1 sample from reaction **5** at 120 °C in air (no inert gas) (**Table 1**).

14
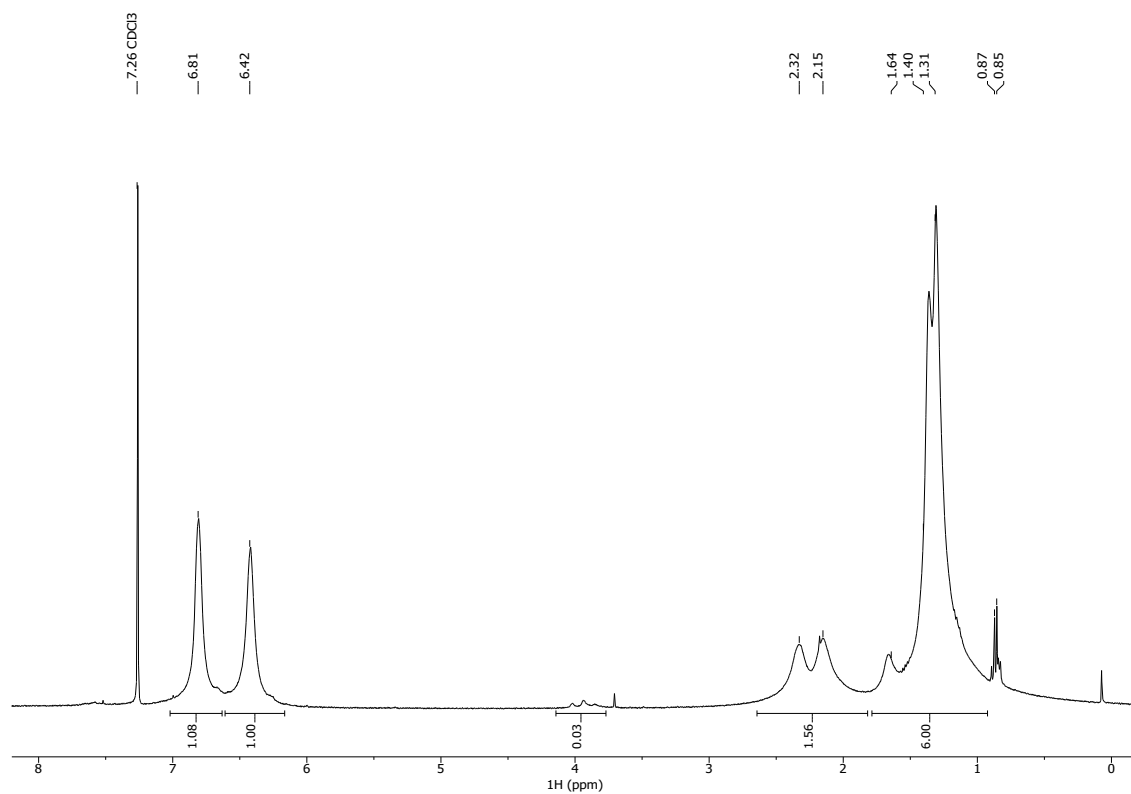
Figure S9. ^{1}H NMR spectrum of PIM-1 sample from larger scale reaction **6** at 160 °C with excess solvent under nitrogen purge (**Table 1**).
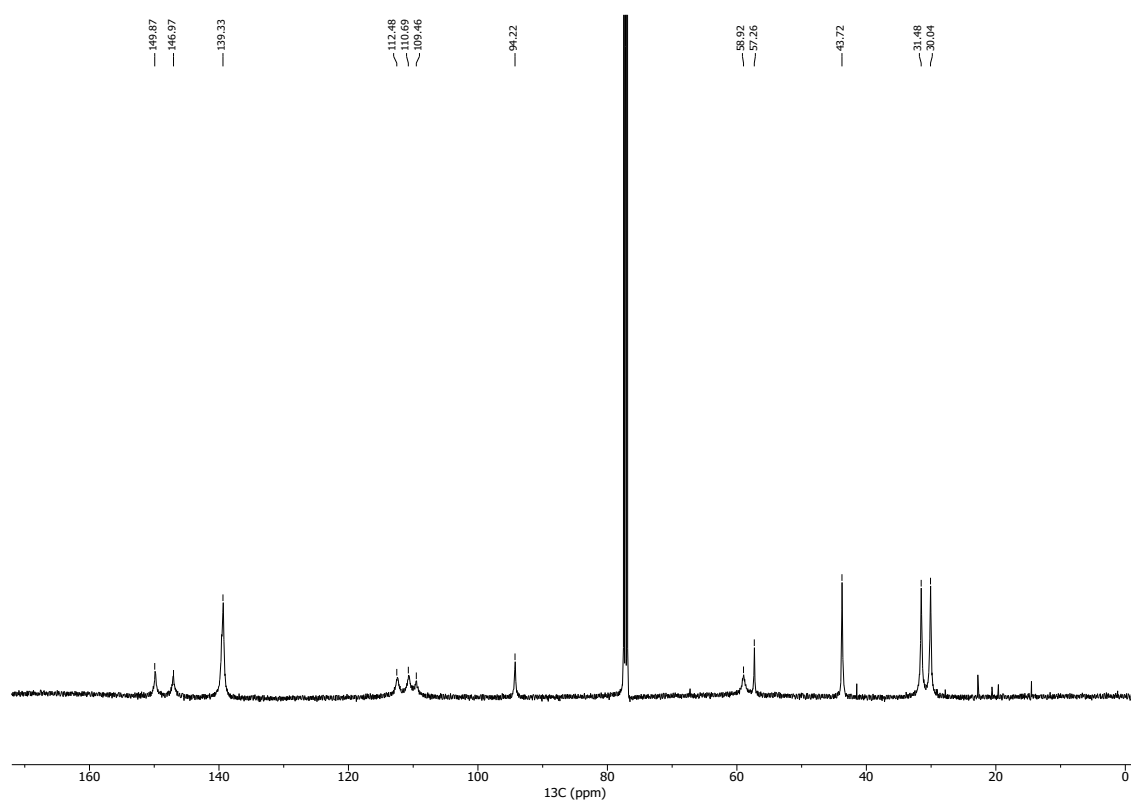
Figure S10. ^{13}C NMR spectrum of PIM-1 sample from larger scale reaction **6** at 160 °C with excess solvent under nitrogen purge (**Table 1**).

S7. Building blocks in early stages of step growth polymerizations of PIM-1.

We assign a green dot to represent a chloro terminated end (**C**) and a red triangle to represent a spiro terminated end (**S**) of a typical PIM-1 oligomeric chain formed in early stages of a step growth polymerization (**Scheme S3**). A purple dot is used to represent the structure associated with a branch point. The blue lines linking the symbols denotes the oligomeric chain found between the structures. The numbers underneath in the example below denote the number of each monomer residue which make up that particular oligomeric arrangement. A black dot introduced later denotes a four-way linkage, network point, which is critical to the formation of large amounts of colloidal network structures which maintain the overall stoichiometry of the sample.
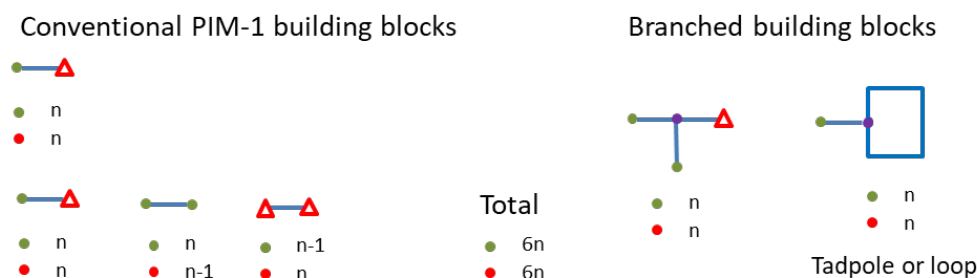
Scheme S3. Representation of oligomeric building blocks.
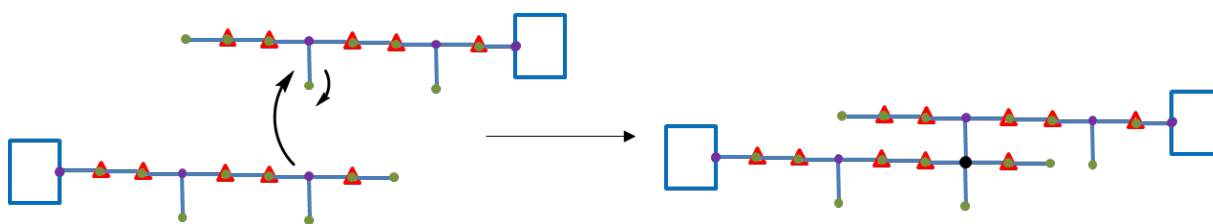
Scheme S4. Example of a secondary reaction between two branched structures to form a network point.

Discussion of step growth polymerization (5) at 120 °C in air.

The elemental analysis of polymer **5** (**Table 2**) indicated the structures formed are far removed from the conventional disubstituted form of the PIM-1 polymer. The molar mass of the majority of the sample is low, yet the C/N ratio for the entire sample is exactly what you would expect for perfect stoichiometry: ratio of TCTPN (**C**) to TTSBI (**S**) monomer derived residues derived from the C/N ratio, [r(**C/S**)] = 1.00. NMR analysis shows that the building blocks of the step growth include the formation of branch points, which each use up an extra spiro unit and generate an extra chloro residue end in the polymer chains formed, maintaining overall stoichiometry in the polymeric structure. This was also confirmed by the excessive amount of chlorine (1.83 %) found in this sample. The amount of chlorine present equates to the presence of only 8.0 spiro (**S**) residues per single chloro (**C**) residue end (2 chlorines).

UV-vis absorption analysis of the reduction in intensity of the peak (433 nm) associated with conjugated sections in a conventional disubstituted PIM-1 sample (polymer **1**), can provide a crude measurement of the number of **S** residues per branch point. For polymer **5**, this peak was diminished by 14 %, which equated to the presence of one branch per every 7.1 **S** residues. We can relate this prediction to the number-average molar mass of the polymer (M_n =10,500) obtained in SEC analysis and calculate the number of branches per average polymer chain for this predominantly soluble polymer sample (85.7 wt %). This determined that there were just over 3 branch points present on an average polymer chain of polymer **5**.

If we consider, to start with, the addition of only the open branched structure to the building block structures expected to constitute the average polymer chain, presented in **Scheme S5**, we know that overall there are equal numbers of both monomeric units in the overall polymer structure, so the ends built on the branched structure reflect that situation. If we then seek to build up a proposed overall structure based on these step growth fragments in proportions which reflect as close as possible the number of branch points per PIM-1 residues, which would be 3 branch points per 24 PIM-1 residues overall, we find that we create a branched structure with a total of 4 chloro terminated ends (8 chlorines in total) and one spiro terminated end. This structure in itself cannot provide a rationale as to why this particular polymeric sample is both low in molar mass and/or contains a network component. Our previous work, which included detailed NMR analysis, concluded that spiro-terminated ends are in reality very rare, and indeed a very large change in the starting stoichiometric balance of the two monomers is required even to generate a spiro-terminated end at all. The elemental analysis of this sample suggested that on average each polymer chain contains only 6 chlorine atoms. We therefore propose that two reactive ends groups join together in the early stages of the polymerization to form a tadpole or loop structure. This action creates an overall equimolar polymer structure which cannot react further in the conventional sense associated with the PIM-1 polymerization and delivers a structure with 3 chloro terminated ends, with 6 chlorine atoms attached. Some secondary reactions between branch points and chloro residue ends on other polymer chains result in the formation of four-way linkages (network points) which aid network formation. Examples of these type of reactions between branched polymer chains are presented in **Scheme S6.**

Conventional PIM-1 building blocks

Branched building blocks

or

- 4
- 4

- 4
- 4

- 4
- 3

- 3
- 4

Total

- 24
- 24

- 3
- 3

- 3
- 3

- 3
- 3

Step growth
polymerization
(**5**)

If only defect is branched unit,

Spiro (**S**) end reacts either via intramolecular cyclization as shown
or forms intermolecular bonds between polymer chains

Polymer **5**
main
product

(85.7 wt %)

Intramolecular cyclization favoured at 120 °C as both molar mass
of polymer and network content low.

Scheme S5. Representation of the formation of products from step growth polymerization (**5**) at 120 °C in air.

Examples of secondary
reactions which generate
four way linkages (●)
required for network
formation

Colloidal network
formation

Polymer **5** network (14.3 wt %)

Network points (four-way linkages) do not disrupt the overall
stoichiometric balance in the network structures
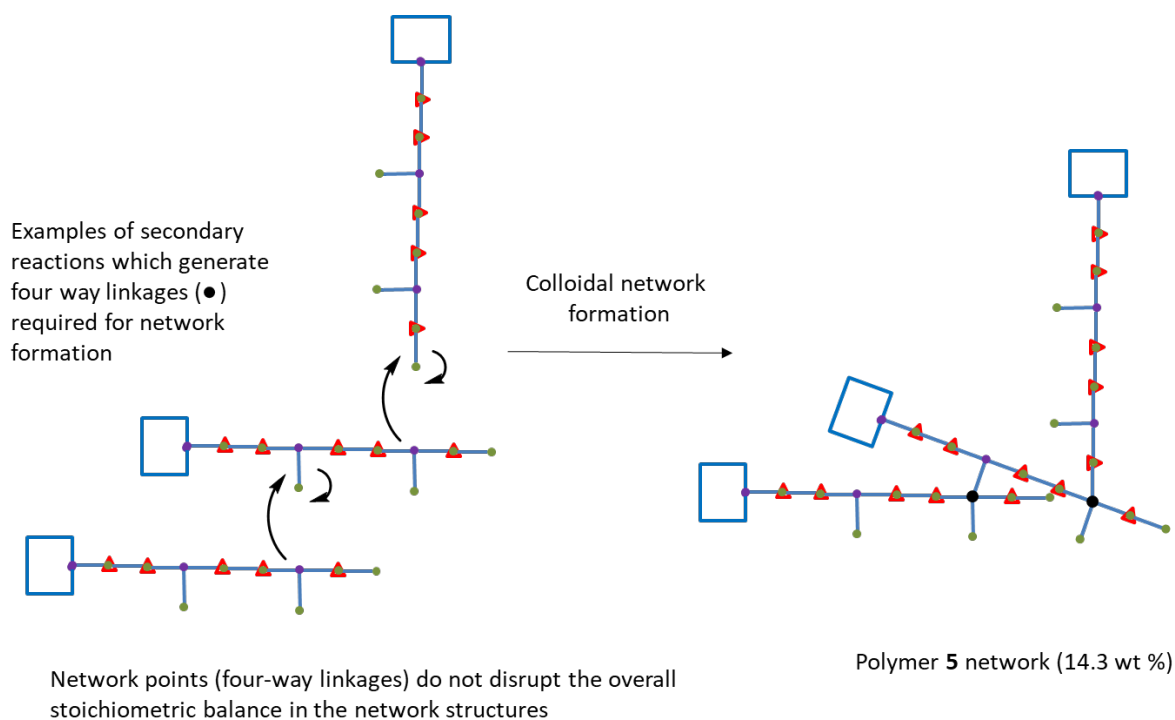
Scheme S6. Examples of secondary reactions between branched structures in polymerization (**5**) at 120 °C in air.

S9. Discussion of step growth polymerization (4) at 140 °C in air.

The elemental analysis of polymer **4** also indicated a C/N ratio reflective of a stoichiometric reaction which still produced a product with a significant amount of chlorine, at 1.31 wt % (**Table 2**). This amount of chlorine present equates to the presence of only 11.6 spiro (*S*) residues per single chloro (*C*) residue end (2 chlorines). However there is a relatively even split between the soluble (53.2 wt %) and network (46.8 wt %) contents for this sample. If we assume, like for polymer **5**, that the network structure of **4** is based around further secondary reactions between branch points on neighbouring chains, there must be chloro-terminated ends remaining in the colloidal network structures.

UV-vis analysis of polymer **4** in solution indicated that the peak associated with conjugated structures had diminished by 10.3 %, which equates to a prediction of one branch per every 9.7 *S* residues. We can again relate this prediction to the number-average molar mass of the polymer obtained in SEC analysis and calculate the number of branches per average polymer chain for the soluble fraction of the polymer sample (53.2 wt %). This determines that there are just under 4 branch points present on each average polymer chain of polymer **4** (**Scheme S7**). If we then seek to build up a proposed overall structure based on these step growth fragments in proportions which reflect as close as possible the number of branch points per PIM-1 residues, which would be 4 branch points per 39 PIM-1 residues overall, we find that we create a branched structure with a total of 5 chloro-terminated ends (10 chlorines in total) and one spiro-terminated end. As was the case with polymer **5**, we propose that the spiro end would rather combine with a neighbouring chloro-terminated end to form a loop. This leaves a predominant product with still 8 chlorines attached, rather than the 6 chlorines predicted in the elemental analysis. However we have yet to factor in that the network component of this sample is significant and each secondary reaction, which contributes to the network structure, removes a further 2 chlorines from the overall sample. At least two such reactions to form four-way structures (network points) are required per polymer chain to generate the network structures drawn in **Scheme S8.** The consequence of just less than half the polymer sample (network content) undergoing secondary reactions is sufficient to lower the overall chlorine content in the sample from 8 to 6 chlorines per average polymer chain, as suggested by the elemental analysis.

Conventional PIM-1 building blocks

Branched building blocks

or

Total
- 39
- 39

Step growth
polymerization
(4)

If only defect is branched unit,

Spiro (**S**) end reacts either via intramolecular cyclization as shown
or forms intermolecular bonds between polymer chains

Polymer **4**
soluble
product

(53.2 wt %)

Intramolecular cyclization still occurs at 140 °C as both molar mass
of polymer and network content still relatively low.

Scheme S7. Representation of the formation of products from step growth polymerization (**4**) at 140 °C in air.

Examples of reactions which generate
four-way structures which start to
build up network structures.

More branch points per polymer
chain increase likelihood of network
formation.
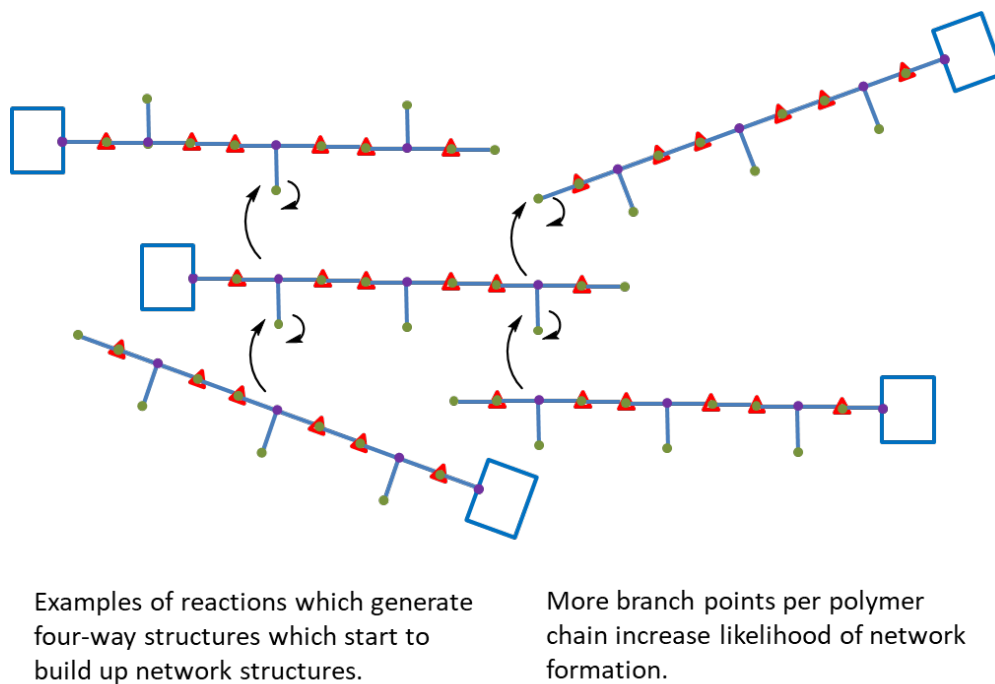
Scheme S8. Examples of secondary reactions between branched structures in polymerization (**4**) at 140 °C in air.

S9. Discussion of step growth polymerization (3) at 160 °C in air.

The elemental analysis of polymer **3** did not register a measurable amount of chlorine (Cl < 0.30 wt %). A lower carbon content than polymer **1**, as found for polymer samples **4** & **5**, can be taken as an indicator that there is some residual chlorine present in polymer **3**. This sample contains a very high percentage of colloidal network material (85.3 wt %). This means that the reaction conditions, 160 °C in air, must favour the secondary reactions to form four-way linkages which remove excess chlorines previously left on the ends of branches.

UV-vis analysis of polymer **3** in solution indicated that the peak associated with conjugated structures had diminished by 8.2 %, which equates to a prediction of one branch per every 12.1 *S* residues. If we then seek to build up a proposed overall structure based on these step growth fragments in proportions which reflect as close as possible the number of branch points per PIM-1 residues, this would be 4 branch points per 51 PIM-1 residues overall (**Scheme 9**). However we have yet to factor in that the network component of this sample is significant and each secondary reaction, which contributes to the network structure, removes a further 2 chlorines (from *C* residue end) from the overall sample, examples of structures formed are presented in **Scheme S9**. Most of the branch points must be converted into network points at this high temperature in air.
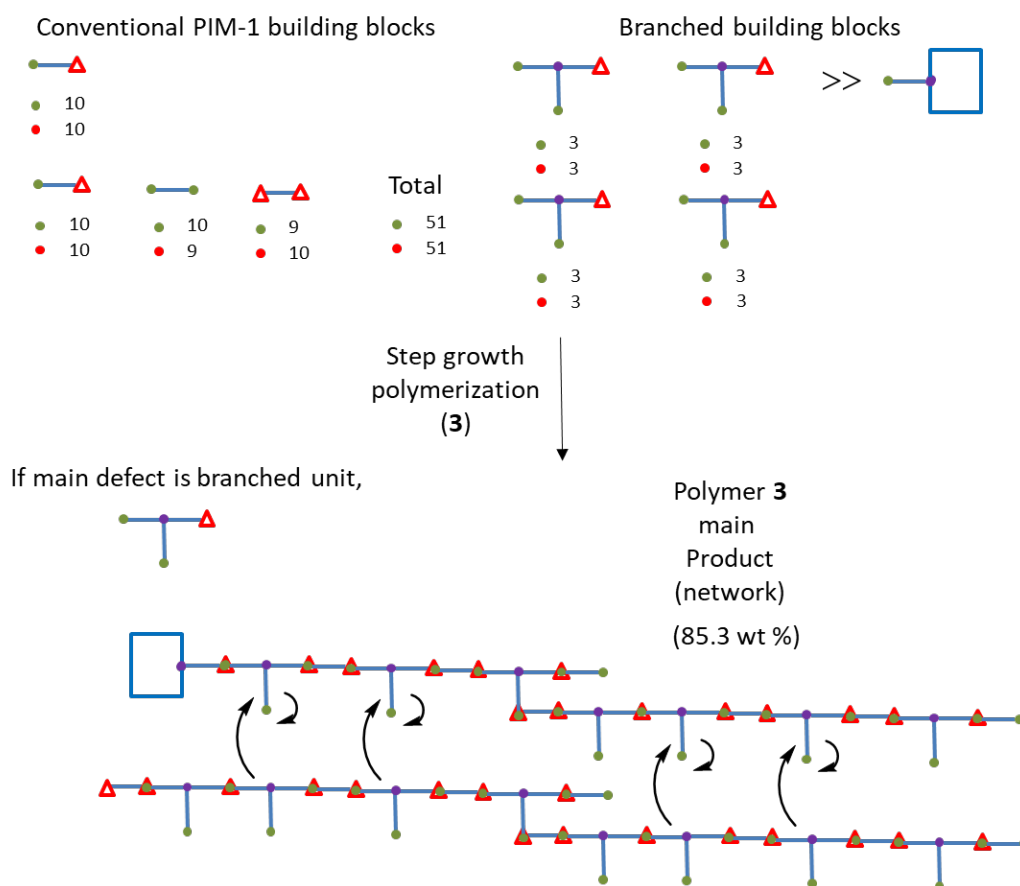
Scheme S9. Representation of the formation of products from step growth polymerization (**3**) at 160 °C in air.
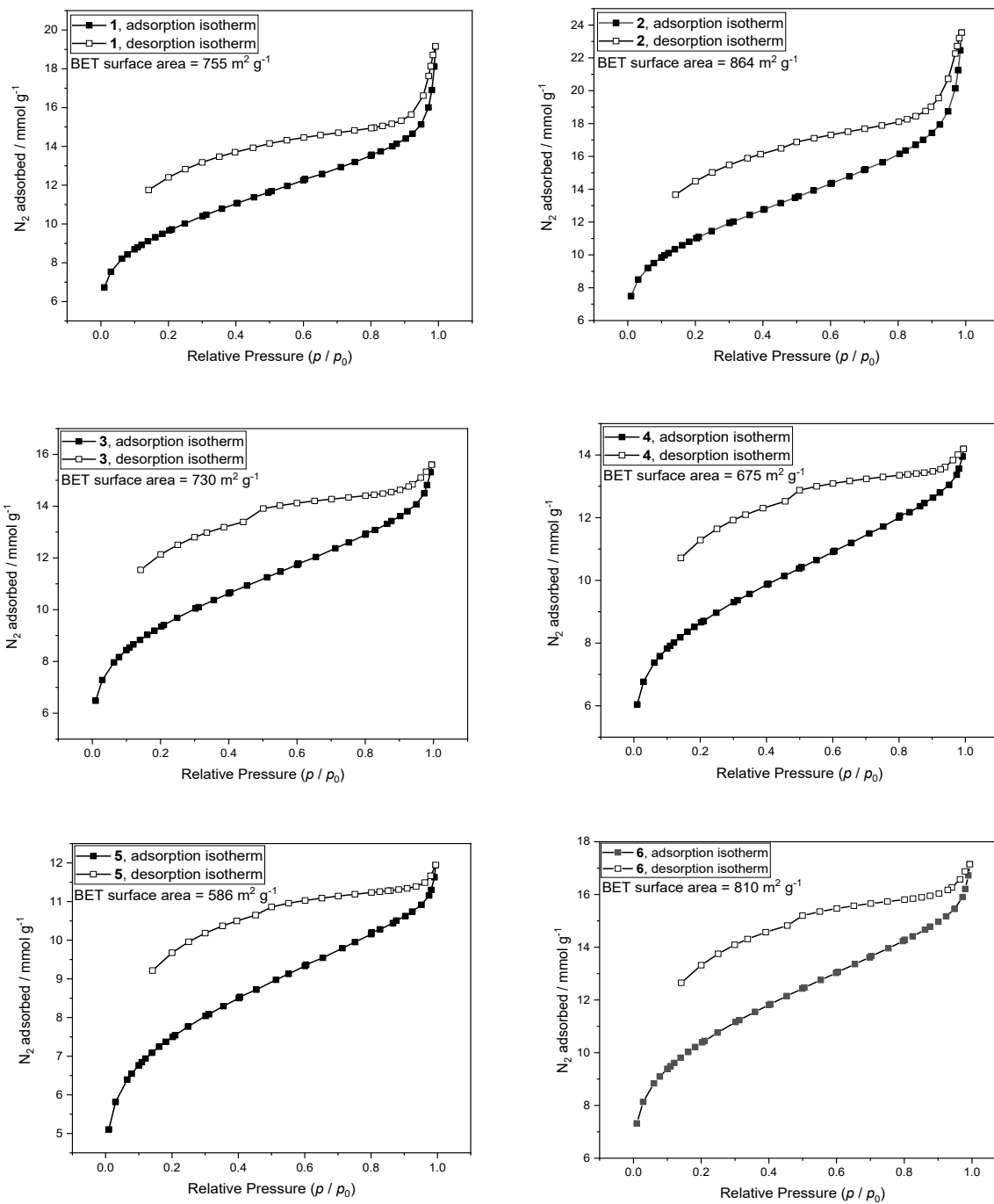
Figure S11. N_2 adsorption and desorption isotherms of PIM-1 polymers, **1-6**, and surface areas from BET analysis.
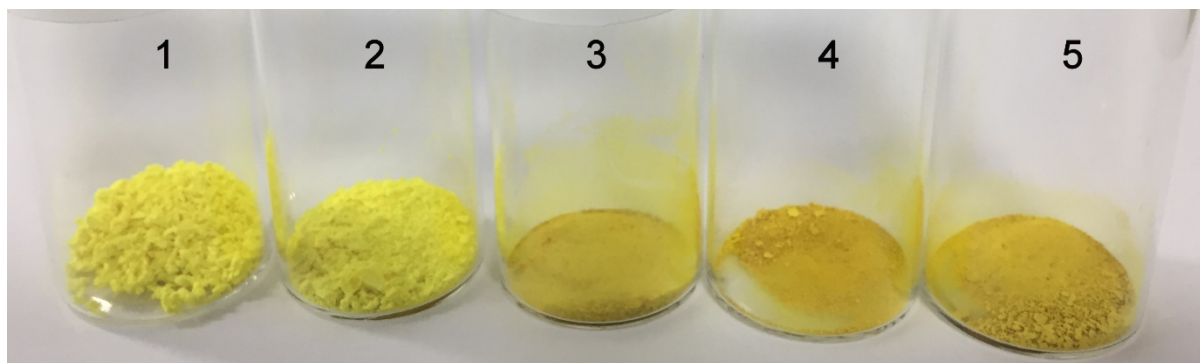
Figure S12. PIM-1 polymer samples (**1-5**).
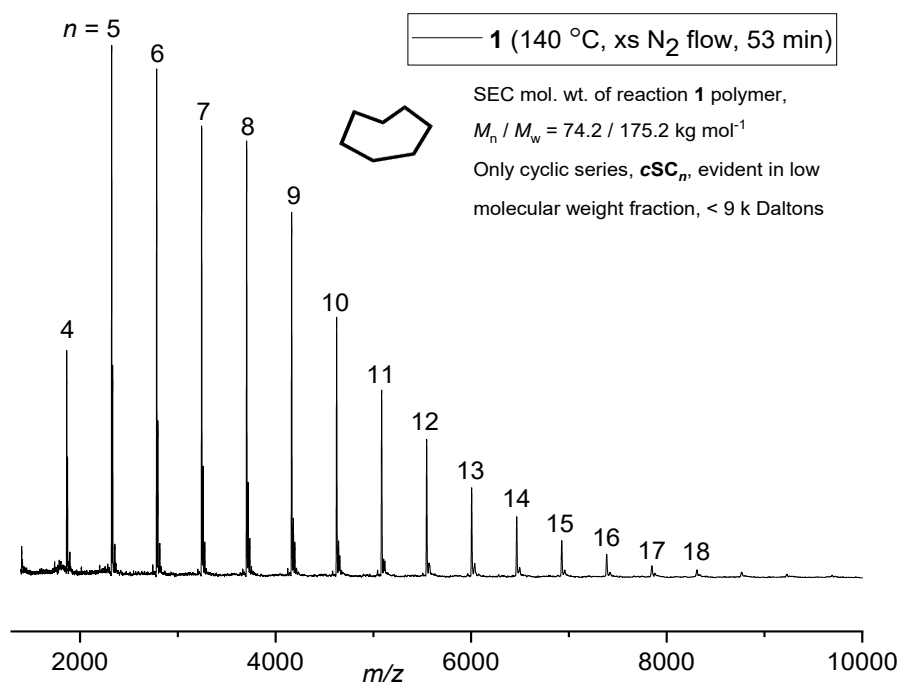
Figure S13. MALDI mass spectrum of PIM-1 sample recovered from excessive nitrogen purge reaction **1** at 140 °C.

The figure shows a MALDI mass spectrum with peaks labeled by n values. The legend reads:

2 (120 °C, xs N_2 flow, 75 min)

SEC mol. wt. of reaction **2** polymer,

M_n / M_w = 69.3 / 156.2 kg mol^{-1}

Only cyclic series, cSC_n, evident in low

molecular weight fraction, < 10 k Daltons

Peaks labeled: $n = 5$, 6, 7, 8, 9, 10, 11, 12, 13, 14, 15, 16, 17, 18, and 4.

x-axis: m/z, with markings at 2000, 4000, 6000, 8000, 10000.
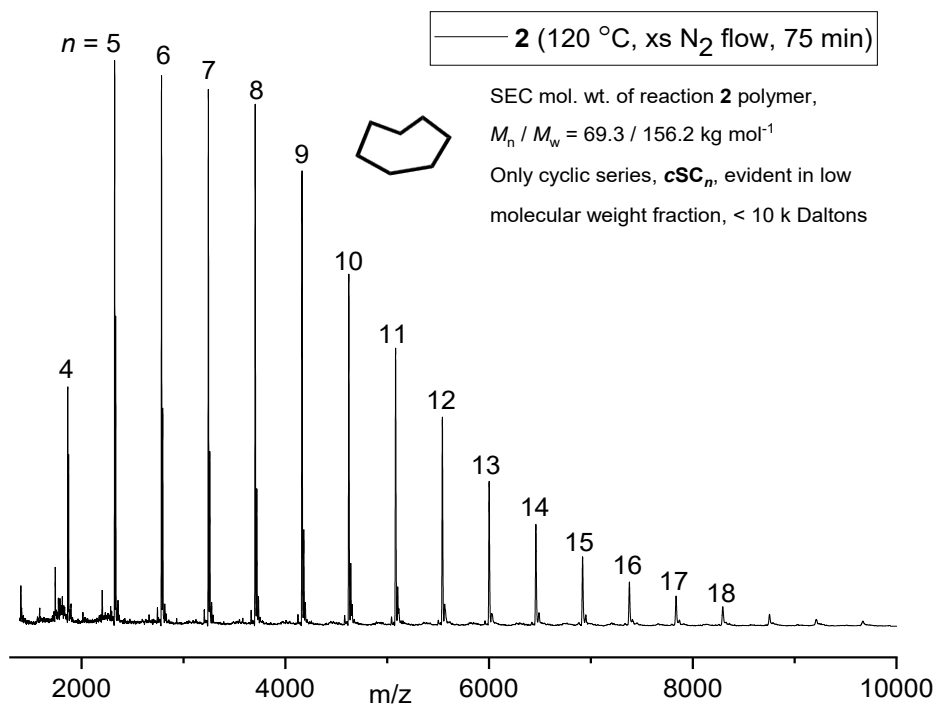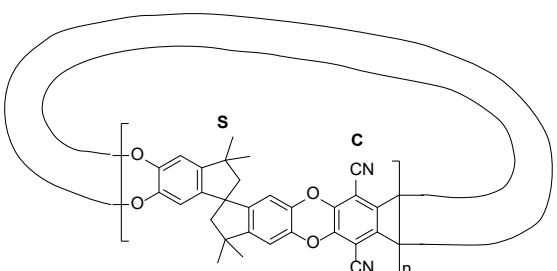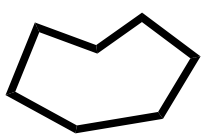
Figure S14. MALDI mass spectrum of PIM-1 sample recovered from excessive nitrogen purge reaction **2** at 120 °C.

Table S1. Predicted adduct masses for cyclic residue (**cSC$_n$**) structures.

Cyclics (cSC$_n$)		Adducts	
		Na$^+$	K$^+$
n	SC$_n$		
1	460.49	483.49	499.49
2	920.98	943.98	959.98
3	1381.47	1404.47	1420.47
4	1841.96	1864.96	1880.96
5	2302.45	2325.45	2341.45
6	2762.94	2785.94	2801.94
7	3223.43	3246.43	3262.43
8	3683.92	3706.92	3722.92
9	4144.41	4167.41	4183.41
10	4604.9	4627.9	4643.9
11	5065.39	5088.39	5104.39
12	5525.88	5548.88	5564.88
13	5986.37	6009.37	6025.37
14	6446.86	6469.86	6485.86
15	6907.35	6930.35	6946.35
16	7367.84	7390.84	7406.84
17	7828.33	7851.33	7867.33
18	8288.82	8311.82	8327.82
19	8749.31	8772.31	8788.31
20	9209.8	9232.8	9248.8
21	9670.29	9693.29	9709.29
22	10130.78	10153.78	10169.78
23	10591.27	10614.27	10630.27
24	11051.76	11074.76	11090.76
25	11512.25	11535.25	11551.25

Table S2. Predicted adduct masses for uneven linear residue (**CC**$_n$) structures terminated on each end with **C** residues derived from TCTPN monomer.

Linear (**CC**$_n$) n	SC$_n$	End groups (+264.1)	Adducts Na$^+$	K$^+$
1	460.49	724.59	747.59	763.59
2	920.98	1185.08	1208.08	1224.08
3	1381.47	1645.57	1668.57	1684.57
4	1841.96	2106.06	2129.06	2145.06
5	2302.45	2566.55	2589.55	2605.55
6	2762.94	3027.04	3050.04	3066.04
7	3223.43	3487.53	3510.53	3526.53
8	3683.92	3948.02	3971.02	3987.02
9	4144.41	4408.51	4431.51	4447.51
10	4604.9	4869	4892	4908
11	5065.39	5329.49	5352.49	5368.49
12	5525.88	5789.98	5812.98	5828.98
13	5986.37	6250.47	6273.47	6289.47
14	6446.86	6710.96	6733.96	6749.96
15	6907.35	7171.45	7194.45	7210.45
16	7367.84	7631.94	7654.94	7670.94
17	7828.33	8092.43	8115.43	8131.43
18	8288.82	8552.92	8575.92	8591.92
19	8749.31	9013.41	9036.41	9052.41
20	9209.8	9473.9	9496.9	9512.9
21	9670.29	9934.39	9957.39	9973.39
22	10130.78	10394.88	10417.88	10433.88
23	10591.27	10855.37	10878.37	10894.37
24	11051.76	11315.86	11338.86	11354.86
25	11512.25	11776.35	11799.35	11815.35

Table S3. Predicted adduct masses for even residue cyclic polymeric structures containing branched PIM-1 residues (**bSC$_n$**).

branched PIM-1, **bSC$_n$**   in larger cyclic structure
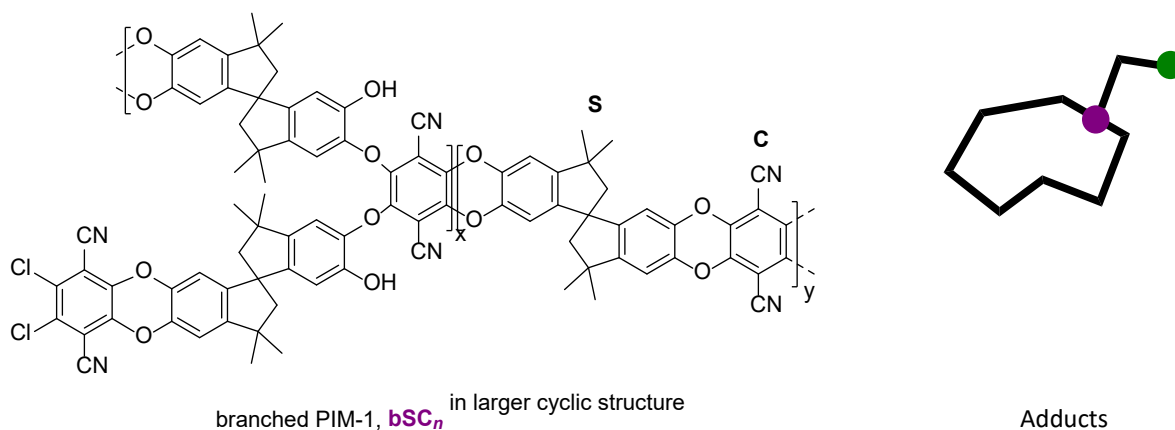
						Adducts	
						Na$^+$	K$^+$
n	x	y	bSC$_x$	SC$_y$	End groups (+0)		
2	1	1	993.03	460.49	1453.52	1476.52	1492.52
3	1	2	993.03	920.98	1914.01	1937.01	1953.01
4	1	3	993.03	1381.47	2374.5	2397.5	2413.5
5	1	4	993.03	1841.96	2834.99	2857.99	2873.99
6	1	5	993.03	2302.45	3295.48	3318.48	3334.48
7	1	6	993.03	2762.94	3755.97	3778.97	3794.97
8	1	7	993.03	3223.43	4216.46	4239.46	4255.46
9	1	8	993.03	3683.92	4676.95	4699.95	4715.95
10	1	9	993.03	4144.41	5137.44	5160.44	5176.44
11	1	10	993.03	4604.9	5597.93	5620.93	5636.93
12	1	11	993.03	5065.39	6058.42	6081.42	6097.42
13	1	12	993.03	5525.88	6518.91	6541.91	6557.91
14	1	13	993.03	5986.37	6979.4	7002.4	7018.4
15	1	14	993.03	6446.86	7439.89	7462.89	7478.89
16	1	15	993.03	6907.35	7900.38	7923.38	7939.38
17	1	16	993.03	7367.84	8360.87	8383.87	8399.87
18	1	17	993.03	7828.33	8821.36	8844.36	8860.36
19	1	18	993.03	8288.82	9281.85	9304.85	9320.85
20	1	19	993.03	8749.31	9742.34	9765.34	9781.34
21	1	20	993.03	9209.8	10202.83	10225.83	10241.83
22	1	21	993.03	9670.29	10663.32	10686.32	10702.32
23	1	22	993.03	10130.78	11123.81	11146.81	11162.81
24	1	23	993.03	10591.27	11584.3	11607.3	11623.3
25	1	24	993.03	11051.76	12044.79	12067.79	12083.79
26	1	25	993.03	11512.25	12505.28	12528.28	12544.28

(n = maximum number of *SC* residues in the cyclic branched structure **bSC$_n$**)

Table S4. Predicted adduct masses for three chloro residue (**C**) terminated linear polymeric structures containing branched PIM-1 residues (**bSC$_n$**).

branched PIM-1, **bSC$_n$**
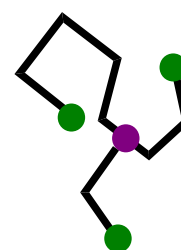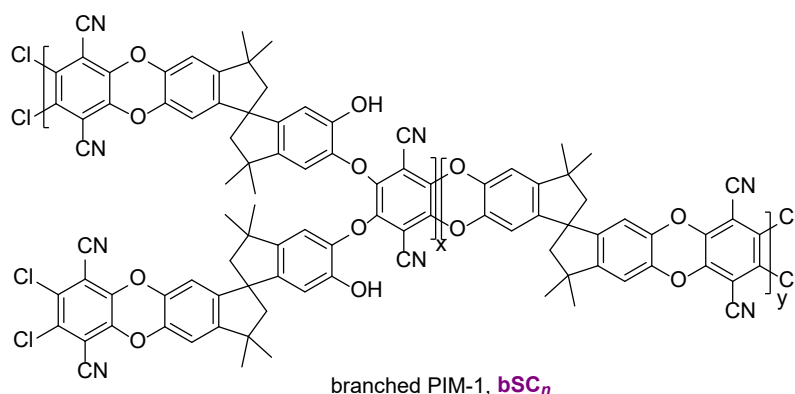
						Adducts	
						Na$^+$	K$^+$
$n*$	x	y	bSC$_n$	SC$_n$	End groups (+140)		
3	1	1	1117.13	460.49	1717.62	1740.62	1756.62
4	1	2	1117.13	920.98	2178.11	2201.11	2217.11
5	1	3	1117.13	1381.47	2638.6	2661.6	2677.6
6	1	4	1117.13	1841.96	3099.09	3122.09	3138.09
7	1	5	1117.13	2302.45	3559.58	3582.58	3598.58
8	1	6	1117.13	2762.94	4020.07	4043.07	4059.07
9	1	7	1117.13	3223.43	4480.56	4503.56	4519.56
10	1	8	1117.13	3683.92	4941.05	4964.05	4980.05
11	1	9	1117.13	4144.41	5401.54	5424.54	5440.54
12	1	10	1117.13	4604.9	5862.03	5885.03	5901.03
13	1	11	1117.13	5065.39	6322.52	6345.52	6361.52
14	1	12	1117.13	5525.88	6783.01	6806.01	6822.01
15	1	13	1117.13	5986.37	7243.5	7266.5	7282.5
16	1	14	1117.13	6446.86	7703.99	7726.99	7742.99
17	1	15	1117.13	6907.35	8164.48	8187.48	8203.48
18	1	16	1117.13	7367.84	8624.97	8647.97	8663.97
19	1	17	1117.13	7828.33	9085.46	9108.46	9124.46
20	1	18	1117.13	8288.82	9545.95	9568.95	9584.95
21	1	19	1117.13	8749.31	10006.44	10029.44	10045.44
22	1	20	1117.13	9209.8	10466.93	10489.93	10505.93
23	1	21	1117.13	9670.29	10927.42	10950.42	10966.42
24	1	22	1117.13	10130.78	11387.91	11410.91	11426.91
25	1	23	1117.13	10591.27	11848.4	11871.4	11887.4
26	1	24	1117.13	11051.76	12308.89	12331.89	12347.89
27	1	25	1117.13	11512.25	12769.38	12792.38	12808.38

($n*$ = total number of **SC** residues in the open branched structure **bSC$_n$**)
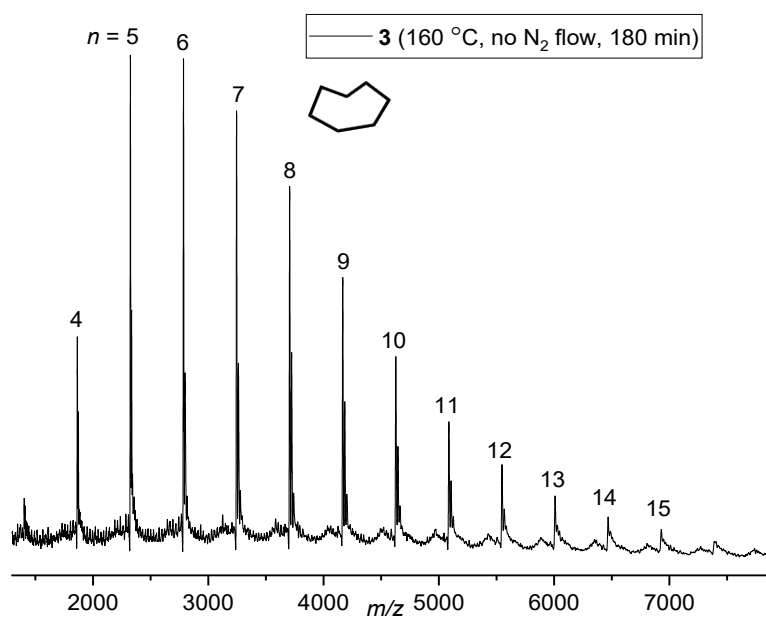
Figure S15. MALDI mass spectrum of PIM-1 sample recovered from no nitrogen purge reaction **3** at 160 °C.
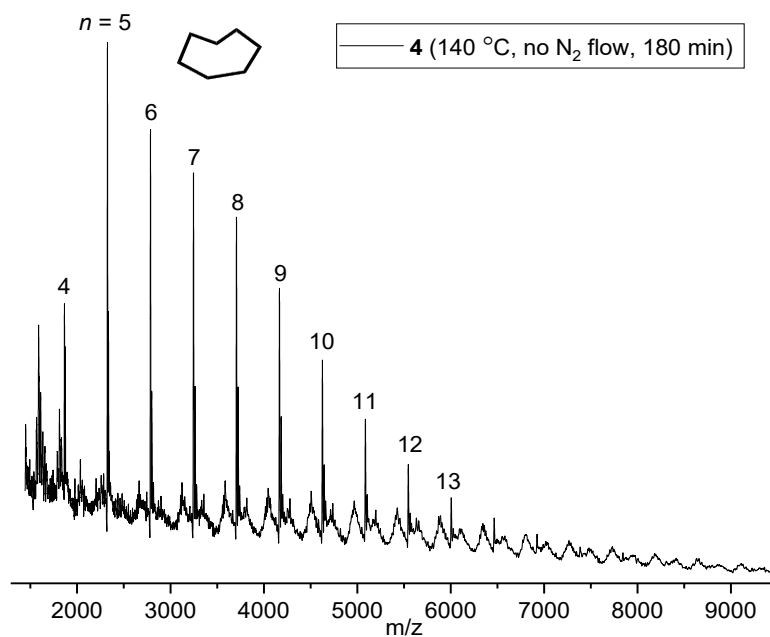
Figure S16. MALDI mass spectrum of PIM-1 sample recovered from no nitrogen purge reaction **4** at 140 °C.
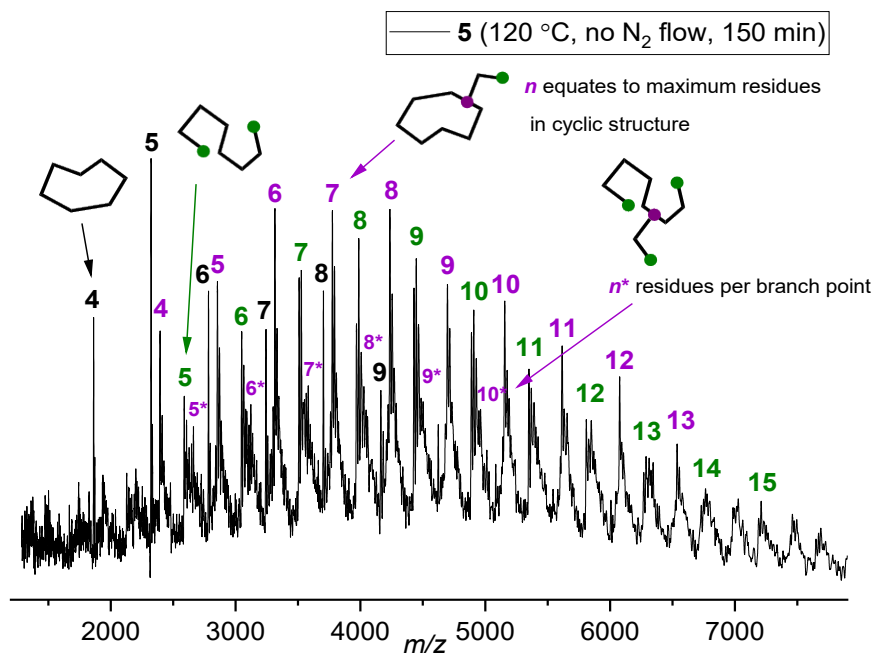
Figure S17. MALDI mass spectrum of PIM-1 sample recovered from no nitrogen purge reaction **5** at 120 °C.

Table S5. Molar attenuation coefficient (ε) values determined from peak maxima (433 nm) of uv-vis absorption spectra of PIM-1 polymers (**1-6**) in THF solutions (0.09 mM). Last four data sets are for four PIM-1 polymers selected from our previous study.[45]

PIM-1 reaction	M_w	M_n	ε / M^{-1} cm^{-1}	Chlorine (Cl) / wt %	Network content / wt %
1	175.2	74.2	9598	< 0.30	0.8
2	156.2	69.3	9684	< 0.30	10.1
3	(8.2)	(5.4)	8807	< 0.30	85.3
4	(23.4)	(16.9)	8609	1.31	46.8
5	14.3	10.5	8252	1.83	14.3
6	62.4	30.5	9014	< 0.30	6.6
2	47.5	30.6	8950	<0.30	0.3
3	58.5	31.3	9506	0.89	3.0
6	8.1	6.2	7660	2.49	2.8
8	12.3	7.6	9347	2.38	n/a
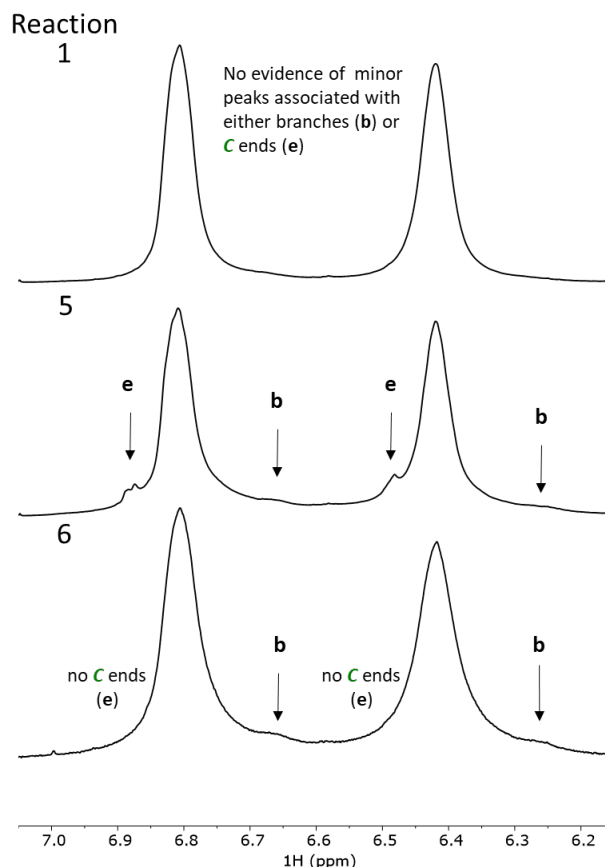
Figure S18. Aromatic proton regions of ^{1}H NMR spectra obtained for polymers, **1**, **5** & **6** in deuterated chloroform.

S11. Discussion of step growth polymerization of refined polymer process (6) under nitrogen purge.

The elemental analysis of polymer **6** did not register a measurable amount of chlorine (Cl < 0.30 wt %). A lower carbon content (C < 74 wt %) than polymer 1, as found for polymer samples **3-5**, can be taken as an indicator that there may be some residual chlorine present. If we consider the detection limit for chlorine, we can qualify this somewhat as < 2.5 chorine atoms potentially present on an average polymer chain. NMR analysis of the aromatic proton region shows branching peaks but no evidence of chloro ended polymeric chains. This suggests that the branched structures are part of loop structures. This sample contains a low level of colloidal network material (6.6 wt %). This suggests that the reaction conditions chosen, under nitrogen, favoured loop formation over secondary reactions which form four-way linkages, which can also remove excess chlorines previously left on the ends of branches. The overall intermediate molar mass obtained in the reaction (M_w = 62,400) would also point to the limitation of branch points not involved in loops.

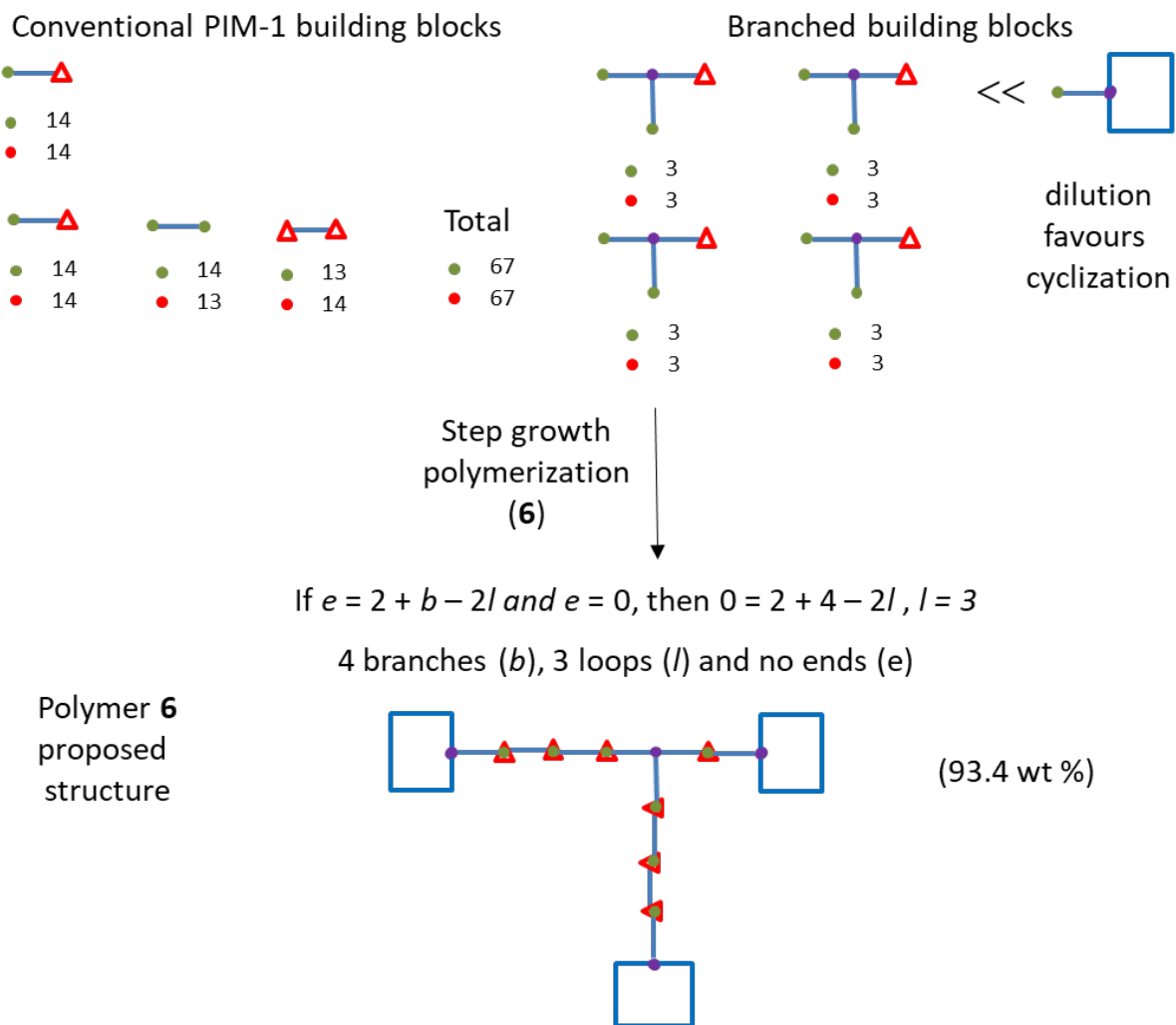UV-vis analysis of polymer 6 in solution indicated that the peak associated with conjugated structures had diminished by 6.1 %, which equates to a prediction of one branch per every 16.4 ***S*** residues. If we then seek to build up a proposed overall structure based on these step growth fragments in proportions which reflect as close as possible the number of branch points per PIM-1 residues, this would equate to 4 branch points per 67 PIM-1 residues overall. A polymeric structure with on average four branch points but 0-1 ends must contain 2-3 loops. A proposed structure is presented in **Scheme S10**. This structure does contain 2 more spiro (***S***) residues than chloro (***C***) residues, which should shift the stoichiometric balance expected in the elemental analysis. However this is a small imbalance within the errors associated with the elemental analysis of a relatively high molar mass polymer. There are many more multiloop structures which can indeed form from 4 branches and show no evidence of end groups, presented in **Scheme S11**.

Conventional PIM-1 building blocks

- 14
- 14

- 14
- 14

- 14
- 13

- 13
- 14

Total
- 67
- 67

Branched building blocks

- 3
- 3

- 3
- 3

- 3
- 3

- 3
- 3

<<

dilution
favours
cyclization

Step growth
polymerization
(**6**)

If $e = 2 + b - 2l$ *and* $e = 0$, then $0 = 2 + 4 - 2l$, $l = 3$

4 branches (*b*), 3 loops (*l*) and no ends (e)

Polymer **6**
proposed
structure

(93.4 wt %)

Note: this structure contains 2 extra spiro (**S**) residues

Scheme S10. Representation of the formation of products from larger scale step growth polymerization (**6**) at average polymerization temperature of 129 °C under nitrogen.
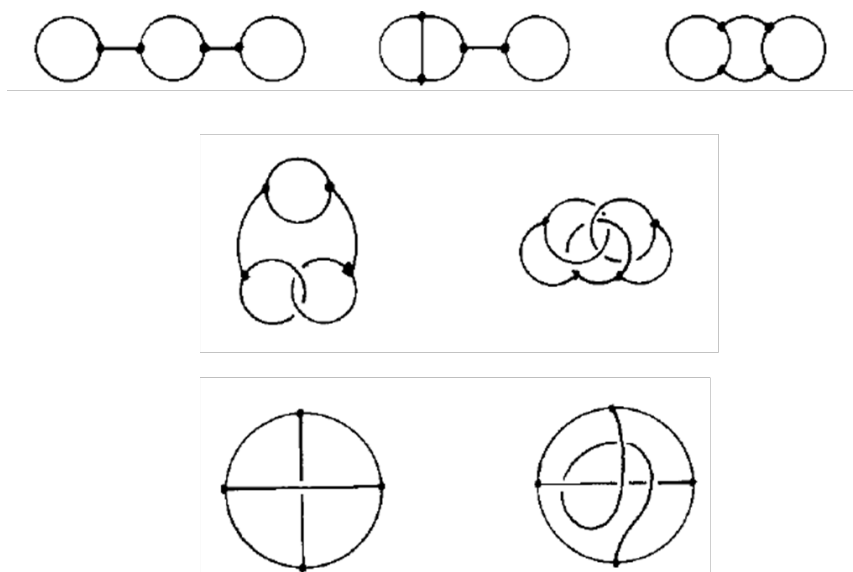
Scheme S11. Other potential loop structures from 4 branches and no ends. Reprinted (adapted) with permission from *Macromolecules* 2000, 33, 17, 6569–6577. Copyright (2000) American Chemical Society. [63]
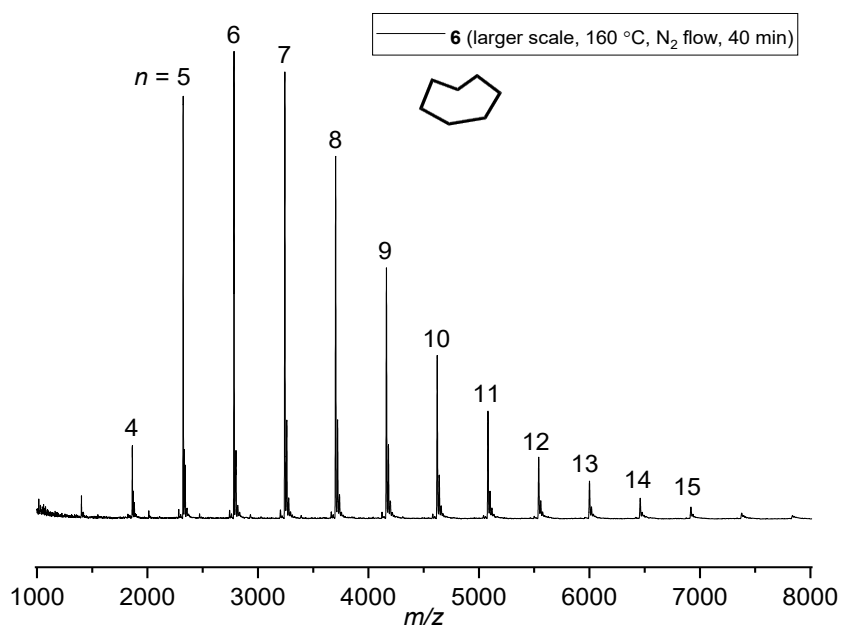
Figure S19. MALDI mass spectrum of PIM-1 sample recovered from larger scale reaction **6** at 160 °C with excess solvent under nitrogen purge (**Table 1**).
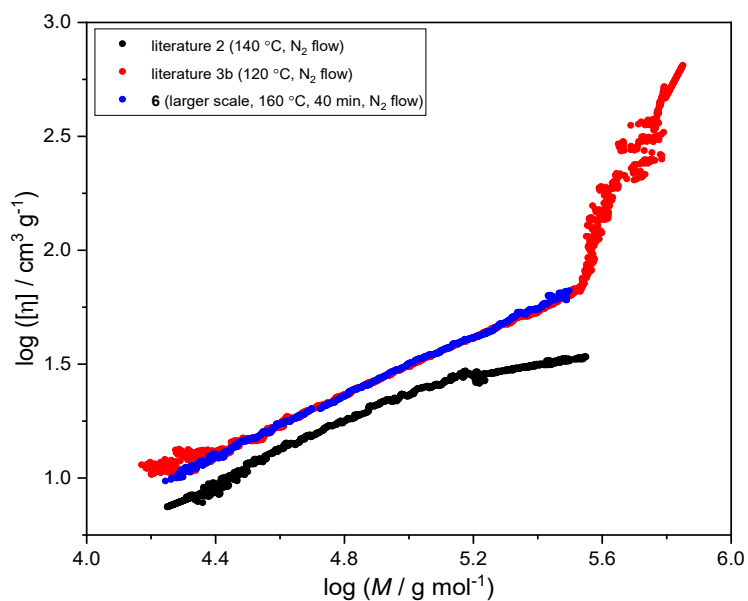
Figure S20. Mark-Houwink plots obtained in multiple detector SEC analysis of polymer **6**, compared against literature samples, 2 and 3b.[45]
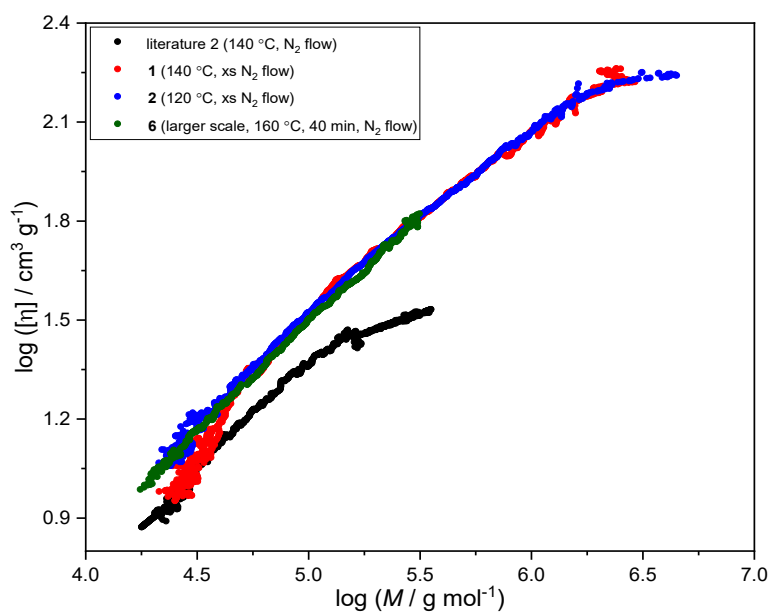
Figure S21. Mark-Houwink plots obtained in multiple detector SEC analysis of polymer **6**, compared against polymers **1**, **2** and literature sample 2.[45]
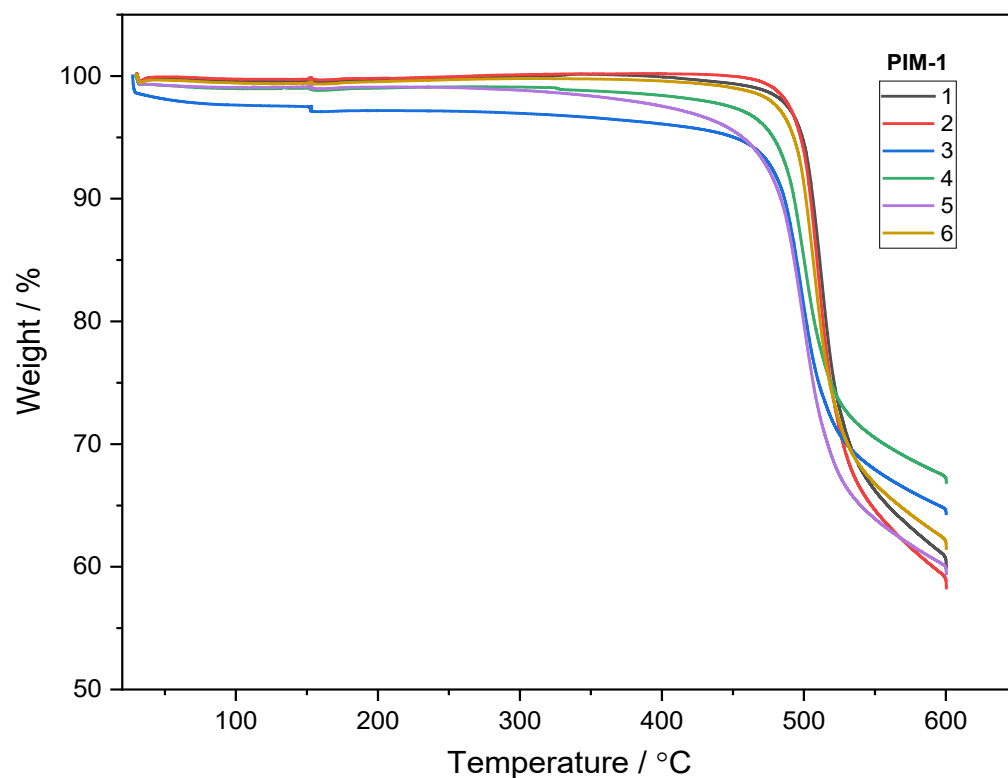
Figure S22. TGA analysis of PIM-1 polymer samples **1-6**. The small drop at 150 °C is associated with an isothermal hold for 1 h.

Table S6. Film thicknesses of active PIM-1 layers cast on top of the PAN support measured from cross sectional TEM analysis of the thin film composite (TFC) membranes.

PIM-1 reaction	M_w	M_n	Network content / wt %	PIM-1 active layer thickness / μm	Layer composition	TFC gas separation performance
1	175.2	74.2	0.8	1.92 (±0.17)	Homogeneous	Selective
2	156.2	69.3	10.1	1.33 (±0.11)	Layered	Selective
3	(8.2)	(5.4)	85.3	∼ 2	Particulate	Knudsen
4	(23.4)	(16.9)	46.8	1.80 (±0.13)	Particulate	Knudsen
5	14.3	10.5	14.3	1.94(±0.22)	Layered/Particulate	Knudsen
6	62.4	30.5	6.6	2.72 (±0.24)	Homogeneous	Selective
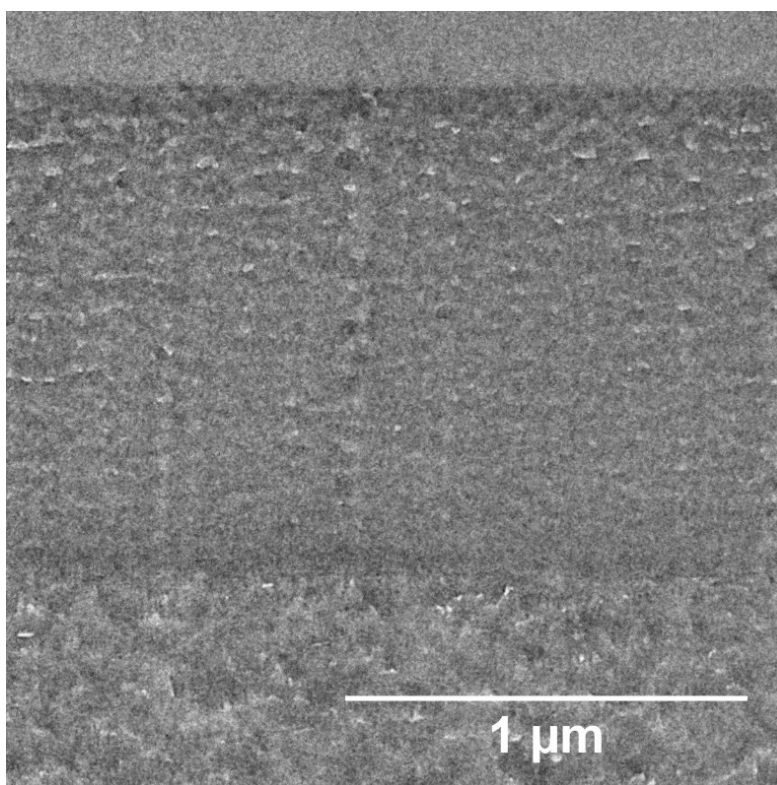
Figure S23. Cross-sectional image of thin film composite membrane of PIM-1 polymer sample **2** obtained in TEM analysis.
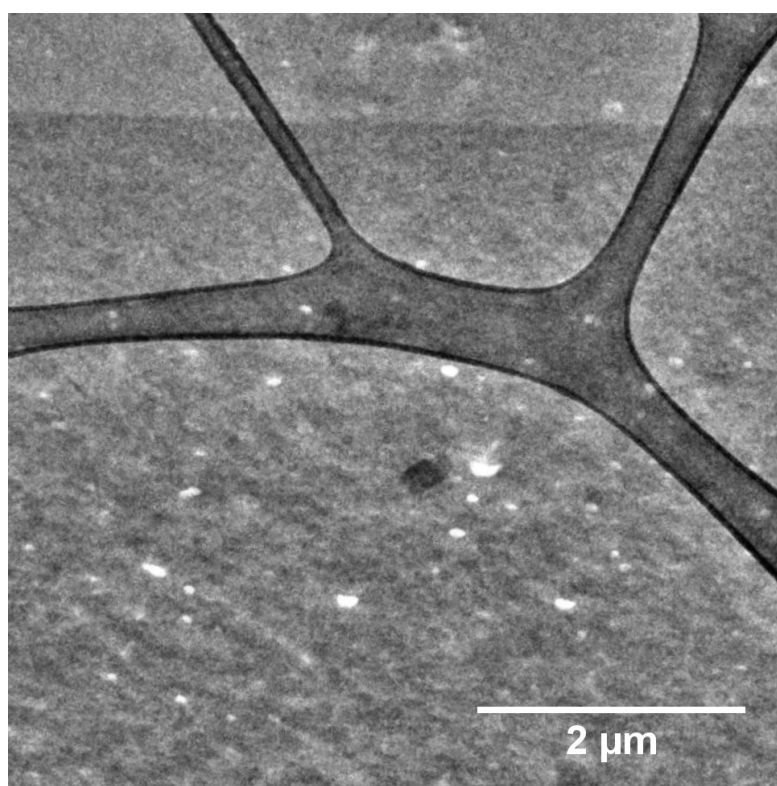
Figure S24. Cross-sectional image of thin film composite membrane of PIM-1 polymer sample **3** obtained in TEM analysis. Selective PIM-1 layer (network rich sample) not very clearly different from the underlying PAN support material.

Figure S25. Cross-sectional image of thin film composite membrane of PIM-1 polymer sample **5** obtained in TEM analysis.

Figure S26. Cross-sectional image of thin film composite membrane of PIM-1 polymer sample **6** obtained in TEM analysis.

Table S7. Single gas (CO_2, N_2) permeation performances of thin film composite membranes (active layer ≤ 2 μm[a]) prepared from the PIM-1 samples (**1-5**).

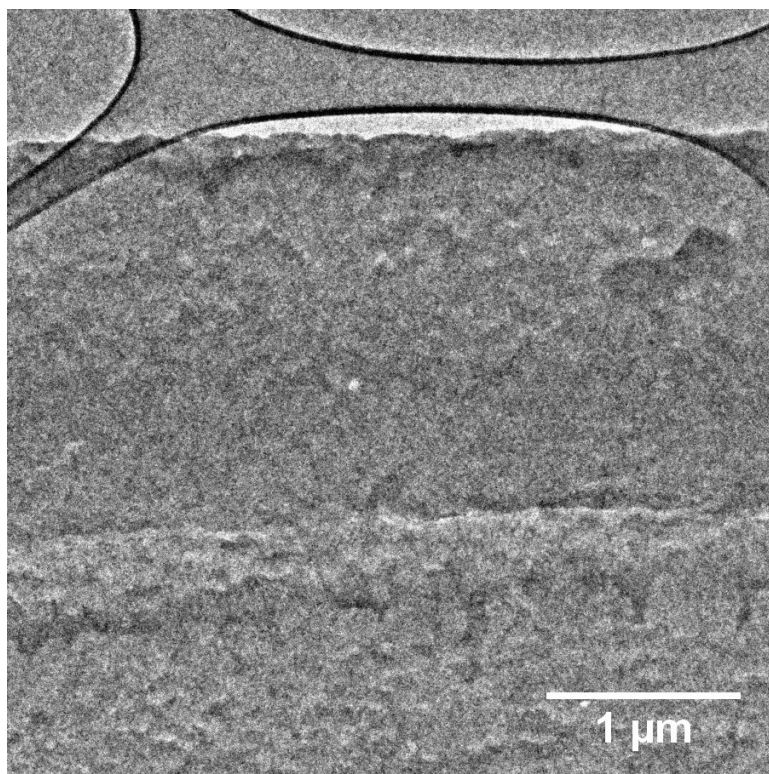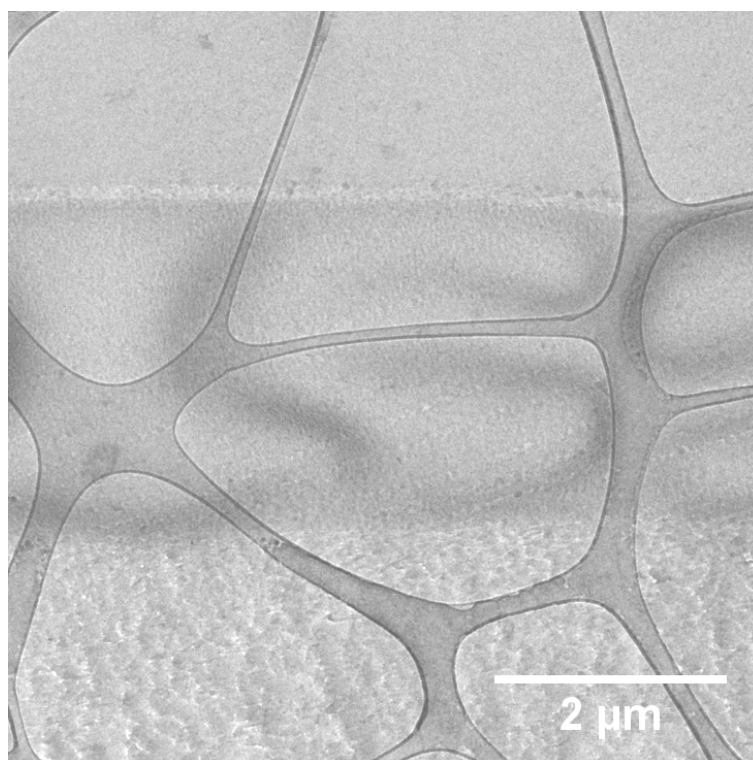| PIM-1 polymer	Reaction conditions[b]	Network PIM-1 content / wt %	Film aging / days	Permeance, K / GPU[c] CO_2	N_2	Selectivity CO_2 / N_2
1	140 °C, xs N_2 purge	0.8	1	4678 (±518)	419 (±61)	11.2
			7	1114 (±144)	96 (±1)	11.7
			28	134 (±28)	37.6 (±28)	3.56
2	120 °C, xs N_2 purge	10.1	1	2903 (±338)	505 (±258)	5.75
			7	4051 (±50)	309 (±47)	14.0
			28	343 (±52)	188 (±41)	1.82
3	160 °C, no N_2 purge	85.3	1	1514 (±333)	804 (±475)	1.88
			7	619 (±193)	817 (±266)	0.76
			28	1337 (±292)	1786 (±517)	0.77
4	140 °C, no N_2 purge	46.8	1	12726 (±4082)	12315 (±5227)	1.03
			7	12207 (±5953)	14554 (±6636)	0.84
			28	13437 (±3146)	19522 (±3715)	0.69
5	120 °C, no N_2 purge	14.3	1	11058	13352	0.83
			7	14154 (±291)	14881 (±1535)	0.95
			28	11492 (±5549)	13072 (±6170)	0.88

[a] PIM-1 active layer thickness, determined via TEM analysis of cross-sections of TFC membranes prepared from each of the samples. Results tabulated in **Table S6**. [b] Polymerization conditions employed to produce PIM-1 samples (**1-5**). The reactions were completed under different nitrogen purge conditions at the set temperatures listed.
[c] 1 GPU = 10^{-6} cm^3 [STP] cm^{-2} s^{-1} cmHg^{-1}.

Table S8. Single gas (CO_2, N_2) permeation performances of thin film composite membranes (active layer ≤ 2 μm[a]) prepared from blend solutions of high molecular weight PIM-1 sample **1** and high network content (85.3 wt %) PIM-1 sample, **3**.

PIM-1 polymer	PIM-1 sample, **3** / wt %	Total blend network PIM-1 content[b] / wt %	Film aging / days	Permeance, K / GPU[c] CO_2	N_2	Selectivity CO_2 / N_2
1	0	0.8	1	4678 (±518)	419 (±61)	11.2
			7	1114 (±144)	96 (±1)	11.7
			28	134 (±28)	37.6 (±28)	3.6
	2	2.5	1	4349 (±367)	305 (±40)	14.3
			7	2504	205	12.2
			28	1129 (±815)	77.7 (±32)	14.5
	10	9.3	1	5410 (±455)	430 (±56)	12.6
			7	2850 (±716)	227 (±5)	12.6
			28	287 (±107)	15.9 (±1)	18.1
	20	17.7	1	5910 (±704)	357 (±49)	16.6
			7	3129 (±848)	183 (±49)	17.1
			28	3480 (±209)	233 (±6)	14.9
			130	34.9 (±10)	3.3 ((±1.6)	10.7
	80	68.4	1	4615 (±1329)	347 (±78)	13.3
			7	4315 (±1613)	1547 (±1247)	2.8
			28	694 (±310)	646 (±247)	1.1
3	100	85.3	1	1514 (±333)	804 (±475)	1.9
			7	619 (±193)	817(±266)	0.8
			28	1377 (±292)	1786 (±517)	0.8

[a] Estimated PIM-1 active blend layer thicknesses, based on TEM analysis of cross-sections of TFC membranes prepared from each of the original samples. Results for **1** and **3** tabulated in **Table S6**. [b] Total network content in the blends was calculated from consideration of the relative proportions of polymer **1** (0.8 wt %) and polymer **3** (85.3 wt %) mixed. The network content present in each sample used in blending will not necessarily have the same topology or cross-linking density. [c] 1 GPU = 10^{-6} cm^3 [STP] cm^{-2} s^{-1} cmHg^{-1}.

Figure S27. Single gas (CO_2, N_2) permeance and selectivity performance after 1 day aging of thin film composite membranes prepared from blends of high molecular weight polymer **1** with high network content sample **3.**

Figure S28. Single gas (CO_2, N_2) permeance and selectivity performance after 7 day aging of thin film composite membranes prepared from blends of high molecular weight polymer **1** with high network content sample **3.**

Figure S29. Single gas (CO_2, N_2) permeance and selectivity performance after 28 and 130 day aging of thin film composite membranes prepared from blends of high molecular weight polymer **1** with high network content sample **3.**

Figure S30. Permeance aging of the individual gases, CO_2 and N_2, through TFC membranes cast from solution blends of PIM-1 polymers, **1** and **3**.

Table S9. Single gas (CO_2, N_2) permeation performances of thin film composite membranes (active layer ≤ 2 μm[a]) prepared from blend solutions of high molecular weight PIM-1 sample **1** and intermediate network content (46.8 wt %) PIM-1 sample, **4**.

PIM-1 polymer	PIM-1 sample, **4** / wt %	Total blend network PIM-1 content[b] / wt %	Film aging / days	Permeance, K / GPU[c] CO_2	N_2	Selectivity CO_2 / N_2
1	0	0.8	1	4678 (±518)	419 (±61)	11.2
			7	1114 (±144)	96 (±1)	11.7
			28	134 (±28)	37.6 (±28)	3.6
	5	3.1	1	7563 (±127)	557 (±13)	13.6
			7	3068 (±406)	127 (±37)	24.3
			28	2770 (±204)	235 (±23)	11.8
			132	489	269	1.8
	10	5.4	1	4708 (±226)	310 (±44)	15.2
			7	2697 (±8)	140 (±21)	19.3
			28	1993 (±1003)	144 (±85)	13.8
			130	76.0	13.8	5.5
	20	10.0	1	4356 (±918)	323 (±38)	13.5
			7	2611 (±1087)	159 (±50)	16.4
			28	2871 (±93)	182 (±11)	15.8
			130	40.7 (±2.2)	3.7 (±0.7)	11.0
4	100	46.8	1	12726 (±4082)	12315 (±5227)	1.0
			7	12207 (±5953)	14554 (±6636)	0.8
			28	13437 (±3146)	19522 (±3715)	0.7

[a] Estimated PIM-1 active blend layer thicknesses, based on TEM analysis of cross-sections of TFC membranes prepared from each of the original samples. Results for **1** and **4** tabulated in **Table S6**. [b] Total network content in the blends was calculated from consideration of the relative proportions of polymer **1** (0.8 wt %) and polymer **4** (46.8 wt %) mixed. The network content present in each sample used in blending will not necessarily have the same topology or cross-linking density. [c] 1 GPU = 10^{-6} cm^3 [STP] cm^{-2} s^{-1} $cmHg^{-1}$.
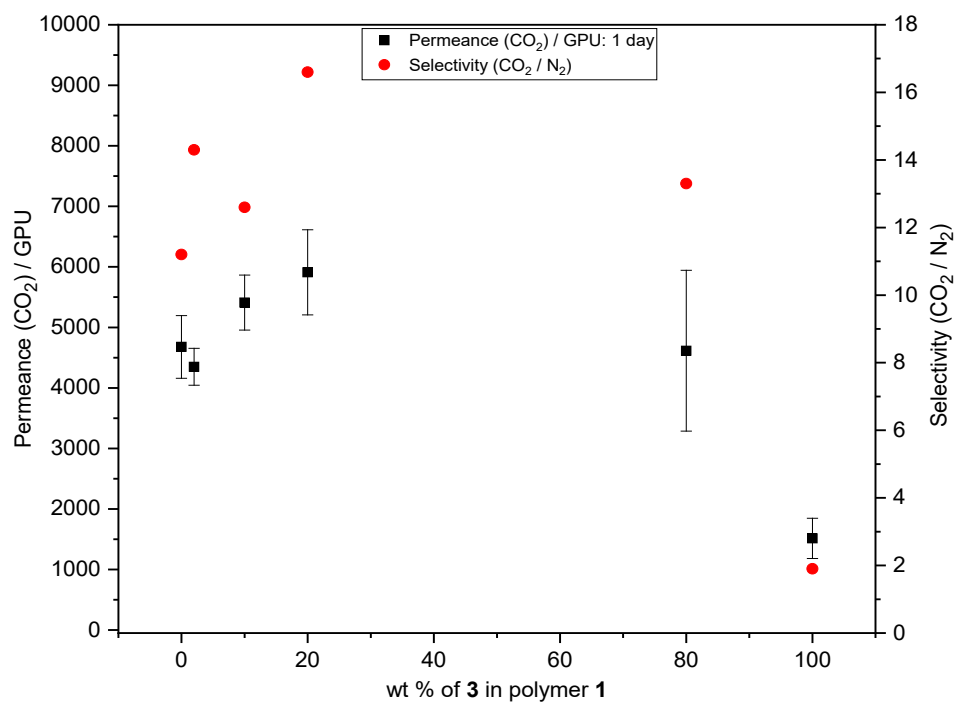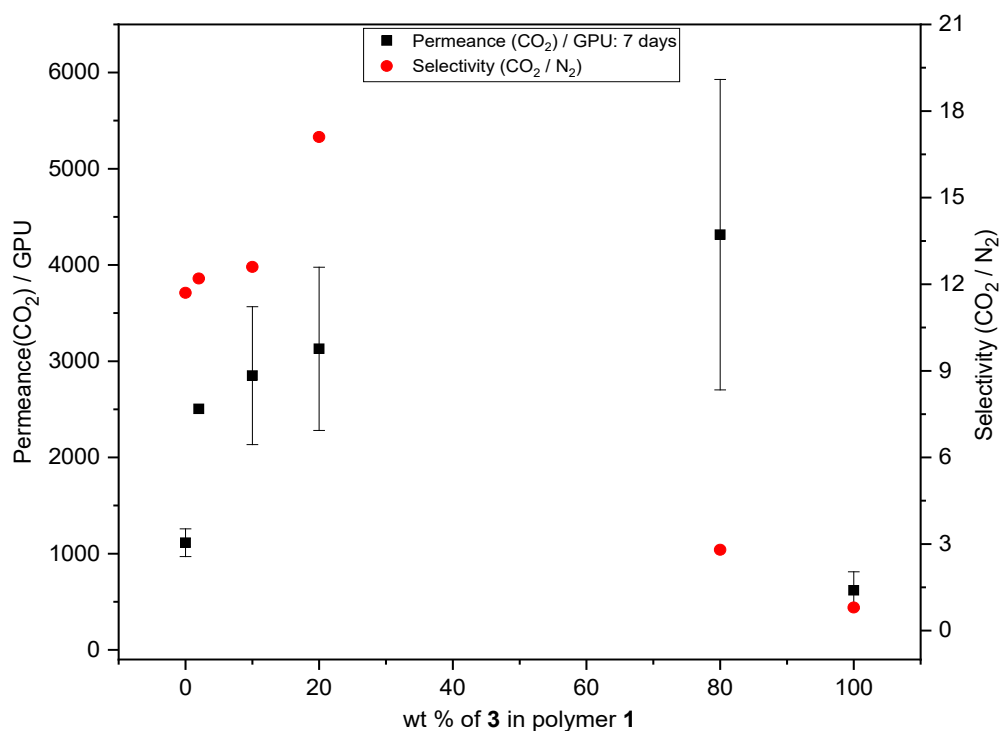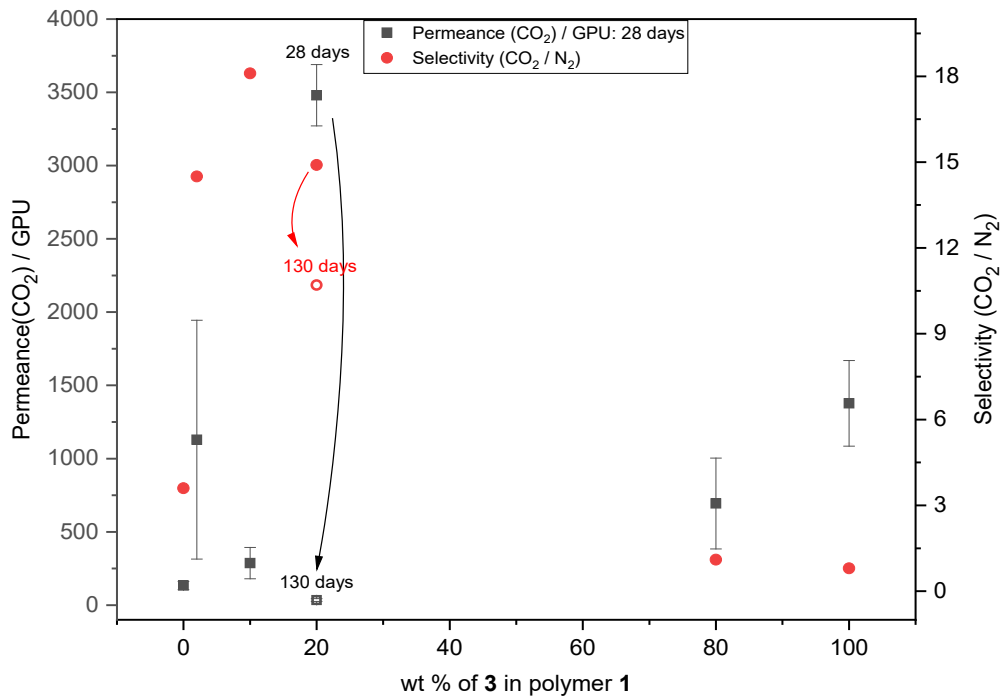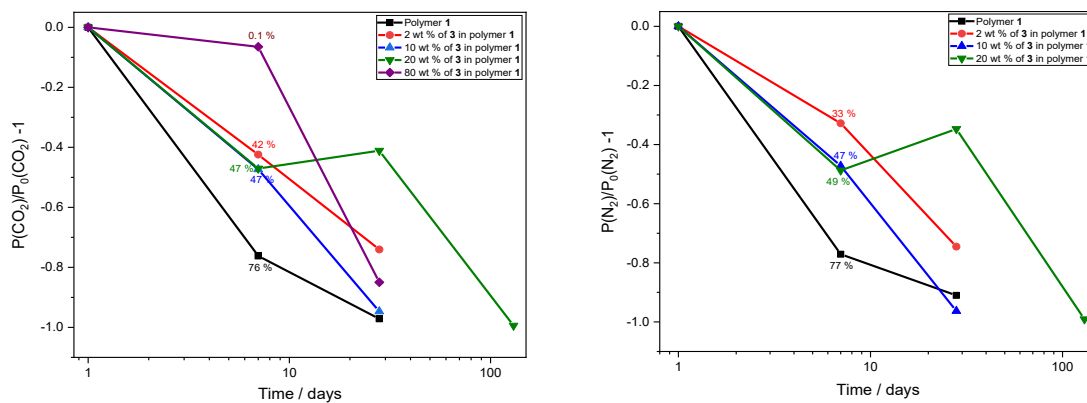

Figure S31. Single gas (CO_2, N_2) permeance and selectivity performance after 1 day aging of thin film composite membranes prepared from blends of high molecular weight polymer **1** with intermediate network content sample **4.**

Figure S32. Single gas (CO_2, N_2) permeance and selectivity performance after 7 day aging of thin film composite membranes prepared from blends of high molecular weight polymer **1** with intermediate network content sample **4.**
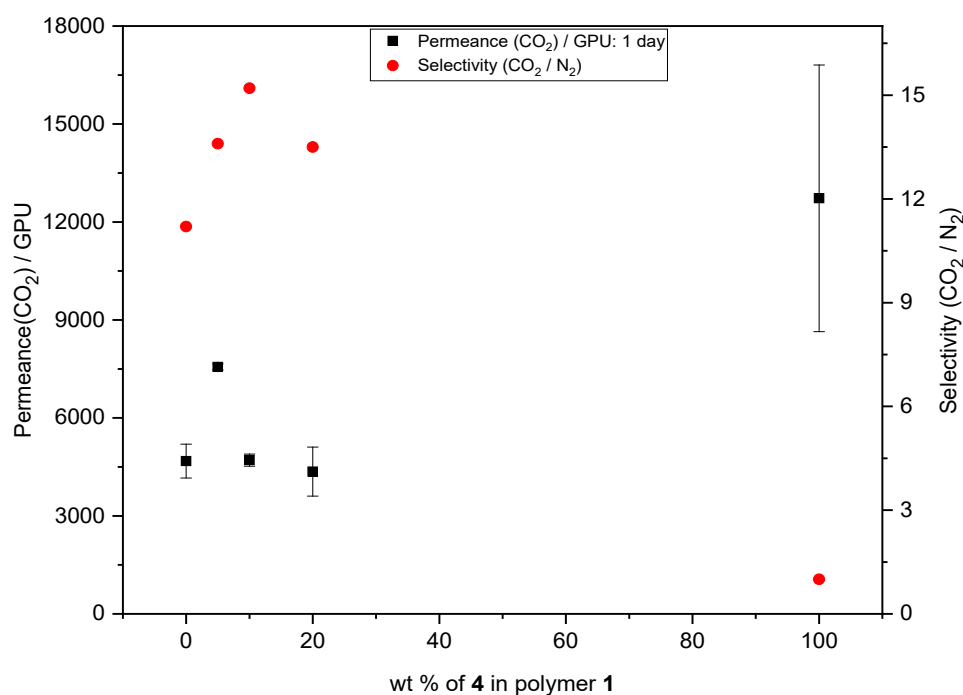

Figure S33. Single gas (CO_2, N_2) permeance and selectivity performance after 28 day aging of thin film composite membranes prepared from blends of high molecular weight polymer **1** with intermediate network content sample **4.**
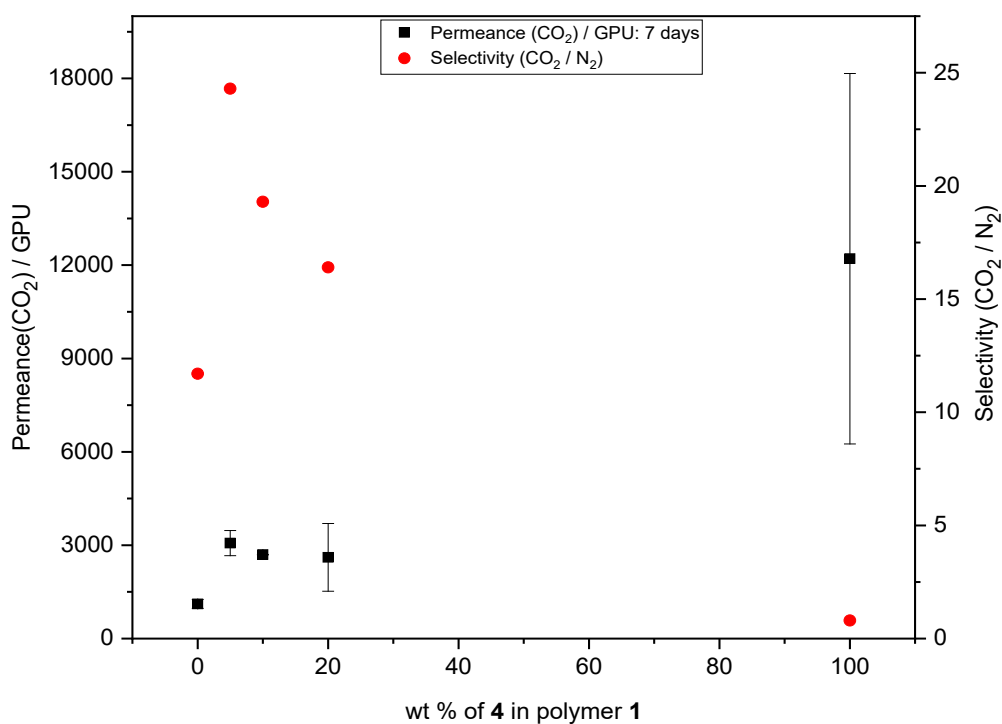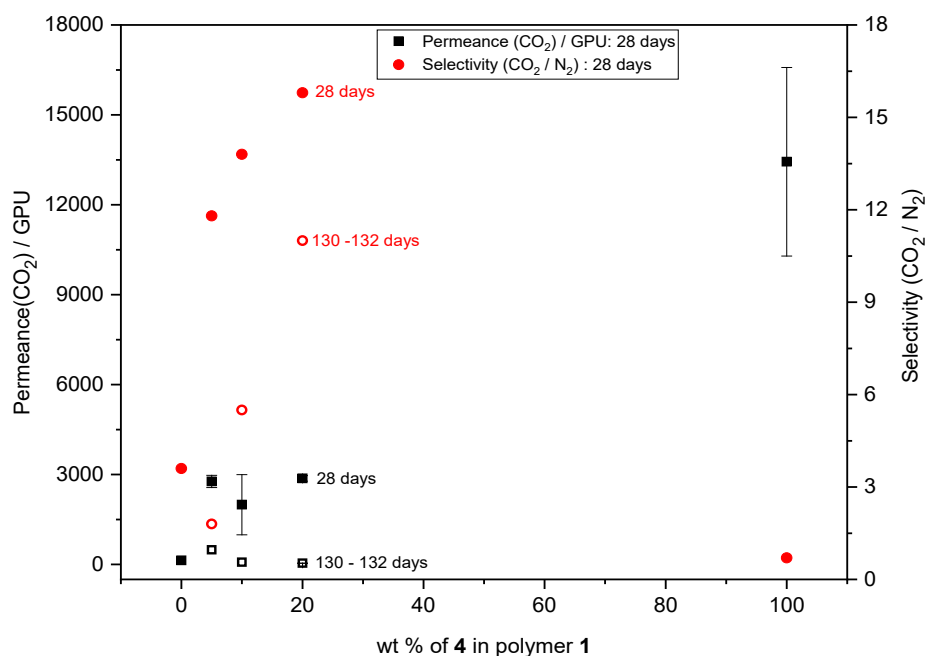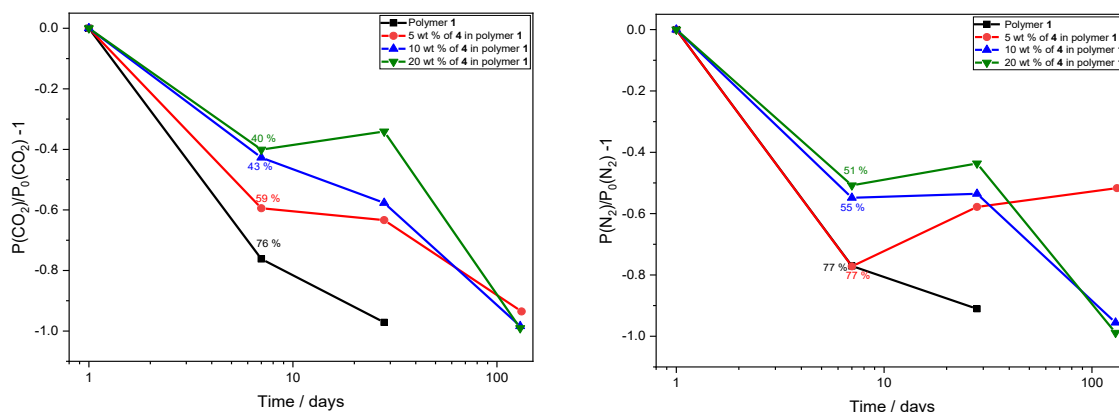
Figure S34. Permeance aging of the individual gases, CO_2 and N_2, through TFC membranes cast from solution blends of PIM-1 polymers, **1** and **4**.

Table S10. Single gas (CO_2, N_2) permeation performances of thin film composite membranes (active layer ≤ 2 µm[a]) prepared from blend solutions of high and low molecular weight PIM-1 samples **2** and **5** (network content, 10.1 and 14.3 % respectively).

PIM-1 polymer	PIM-1 sample, **5** / wt %	Total blend network PIM-1 content[b] / wt %	Film aging / days	Permeance, K / GPU[c]		Selectivity
				CO_2	N_2	CO_2 / N_2
2	0	10.1	1	2903 (±338)	505 (±258)	5.8
			7	4051 (±50)	309 (±47)	13.1
			28	343 (±52)	188 (±41)	1.8
	2	10.2	1	4514 (±650)	754 (±188)	6.0
			7	2613 (±129)	129 (±10)	20.3
	10	10.5	1	4261 (±399)	333 (±13)	12.8
			7	2687 (±16)	198 (±72)	13.6
			625	230	288	0.8
	20	10.9	1	5957 (±993)	454 (±91)	13.1
			7	4418 (±2920)	374 (±327)	11.8
			28	115 (±64.8)	82.5 (±81.3)	1.4
	80	13.5	1	8520 (±2848)	6139 (±3101)	1.4
			7	9620 (±3226)	12671 (±3500)	0.8
			132	5174	6304	0.8
5	100	14.3	1	11058	13352	0.8
			7	14154 (±291)	14881 (±1535)	0.9
			28	11492 (±5549)	13072 (±6170)	0.9

[a] Estimated PIM-1 active blend layer thicknesses, based on TEM analysis of cross-sections of TFC membranes prepared from each of the original samples. Results for **2** and **5** tabulated in **Table S6**. [b] Total network content in the blends was calculated from consideration of the relative proportions of polymer **2** (10.1 wt %) and polymer **5** (14.3 wt %) mixed. The network content present in each sample used in blending will not necessarily have the same topology or cross-linking density. [c] 1 GPU = 10^{-6} cm^3 [STP] cm^{-2} s^{-1} cmHg^{-1}.
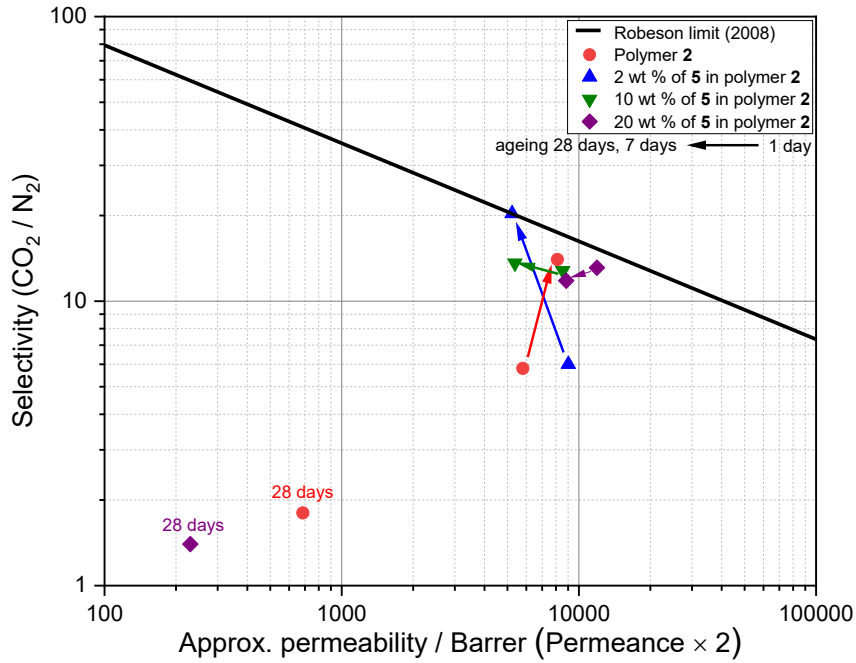
Figure S35. Single gas (CO_2, N_2) permeation performances of the thin film composite membranes (estimated 2 µm selective layer) prepared from blends of high and low molecular weight PIM-1 samples **2** and **5** (network content, 10.1 and 14.3 % respectively).

Figure S36. Permeance aging of the individual gases, CO_2 and N_2, through TFC membranes cast from solution blends of PIM-1 polymers, **2** and **5**.
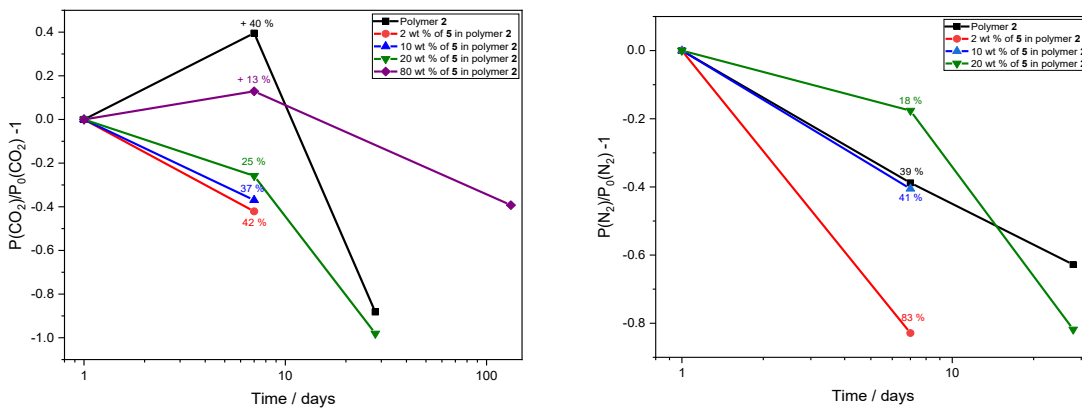
Table S11. Single gas (CO_2, N_2) permeation performances of thin film composite membranes (≤ 2 μm active layer) prepared from literature polymer **3b**, blends of **3b** with some network-rich samples, and polymer **6** itself.

PIM-1 polymer	Network PIM-1 sample, wt %	Total network PIM-1 content[c] / wt %	Film aging / days	Permeance, K / GPU[d]		Selectivity
				CO_2	N_2	CO_2 / N_2
3b	none,-[a]	7.8	1	5985 (±572)	303 (±5)	19.9
			7	1648 (±583)	82 (±18)	20.0
			28	493 (±126)	35 (±0.6)	14.1
	none, -[b]	7.8	1	7323 (±674)	566 (±68)	12.3
			2	3637 (±329)	157 (±27)	23.2
			3	2476 (±381)	109 (±24)	22.6
			7	5389	109	49.6
				2906	72	40.1
				2852	71	40
			14	646 (±540)	81 (±57)	8.0
	3, 10[c]	15.6	1	5732 (±137)	340 (±39)	16.9
			7	5757	122	47.1
				4737	294	16.1
			28	577 (±47)	79 (±40)	7.3
	4, 10[c]	11.7	1	5689 (±1035)	471 (±78)	12.1
			7	5757 (±1042)	511 (±187)	11.3
			28	243 (±105)	71 (±67)	3.4
	4, 20[c]	15.6	1	4635 (±1700)	357 (±156)	13.0
			7	5727 (±1022)	724 (±146)	7.9
			28	344 (±265)	301 (±385)	1.1
	5, 10[c]	8.5	1	3979 (±240)	251 (±28)	15.9
			7	2498 (±65)	120 (±16)	20.9
6	none, -	6.6	1	4642 (±183)	350 (±24)	13.3
			7	1355	44.6	30.4
			28	878 (±295)	32 (±10)	27.6
			120	671 (±59)	25 (±2.1)	26.7

[a] Original single gas permeation analysis of TFC membranes prepared from literature polymer, **3b**. The PIM- 1 active layer was measured as 1.9 (±0.3) μm, based on TEM analysis of cross-sections of the TFC membranes prepared from this sample.[45] [b] Further TFC permeation analysis of polymer **3b**. [c] Total network content in the blends was calculated from consideration of the relative proportions of polymer **3b** (7.8 wt %) and the 'network' polymer blended with it. The network content present in each sample used in blending will not necessarily have the same topology or cross-linking density. [d] Blends of polymer **3b** with the network samples **(3-5)** are attributed 2 μm active layer thicknesses when GPU values were converted into Barrer for the associated Robeson plots (**Figure 12**). 1 GPU = 10^{-6} cm^3 [STP] cm^{-2} s^{-1} $cmHg^{-1}$.
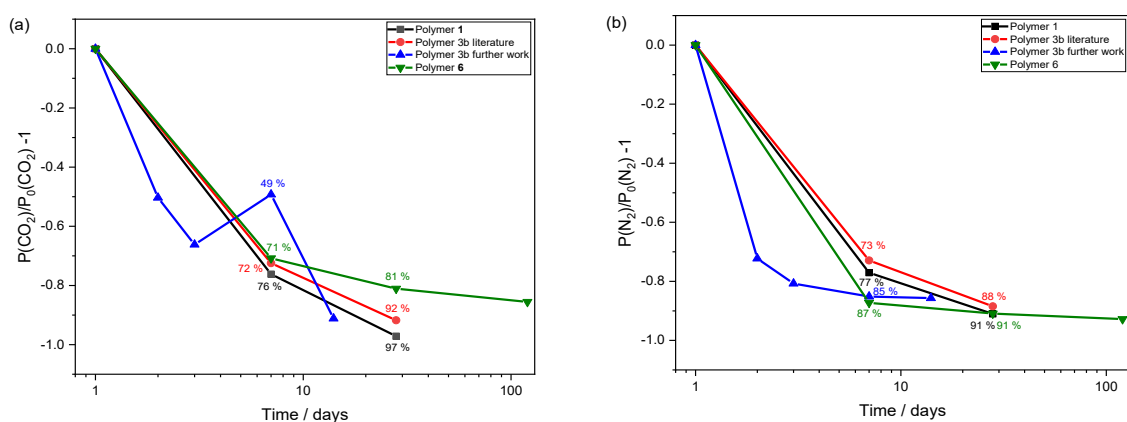

Figure S37. Comparison of permeance aging of the individual gases, (a) CO_2 and (b) N_2, through TFC membranes cast from PIM-1 polymers, **1**, literature 3b and **6**.

S12. Preparation of self-standing PIM-1 film cast from polymer 6 in chloroform.

A self-standing PIM-1 film was cast in a PTFE Petri dish (6 cm) from 3% w/v solution in chloroform (0.12 g of polymer **6** in 4 mL of $CHCl_3$). The solution was filtered through glass wool to ensure that any large aggregates were removed from the solution prior to film formation. Each solution was left for 3 days at room temperature in a nitrogen atmosphere cabinet to allow the film to slowly form and dry. The formed film was then detached from the surface of the Petri dish and soaked in methanol (30 mL) overnight. Methanol supernatant was then removed, and the film placed back in the N_2 cabinet to dry for 2 days at room temperature. The film was then placed in a vacuum oven at 105 °C for 24 h. After oven treatment, test coupons were made up (active membrane area of each coupon cut from the film was 2.84 cm^2) and this was classed as day 1 of testing. The film thickness was measured using a Mitutoyo digital micrometer, with the thickness recorded from an average value obtained from six different points on the respective film.